SIAM J. MATH. ANAL.
Vol. 44, No. 1, pp. 405–436

STANDING WAVES FOR PHASE TRANSITIONS IN A SPHERICALLY SYMMETRIC NOZZLE*

HAITAO FAN† AND XIAO-BIAO LIN‡

Abstract. We study the existence of standing waves for liquid/vapor phase transition in a spherically symmetric nozzle. The system is singularly perturbed and the solution consists of an internal layer where the liquid quickly becomes vapor. Using methods from dynamical systems theory, we prove the existence of the internal layer as a heteroclinic orbit connecting the liquid state to the vapor state. The heteroclinic orbit is reproduced numerically and is also shown numerically to be a transversal heteroclinic orbit. The proof of the existence of an exact standing wave solution near the singular limit is based on the geometric singular perturbation theory and is outlined in the paper.

Key words. liquid/vapor phase transition, spherically symmetric nozzle, internal layer solution, singular perturbation, numerical shooting method

AMS subject classifications. 35B25, 35Q35, 34E15, 65P99

DOI. 10.1137/11082213X

1. Introduction. In this paper, we study the spherically symmetric flow of liquid fuel which mimics the fuel being injected into the cylinder of an internal combustion engine through a cone-shaped nozzle. We investigate the evaporation of liquid fuel in the nozzle and show that under certain conditions a steady evaporation front can occur inside the nozzle so that the fuel emerging from the injection nozzle is in its vapor state. In this way, the fuel vapor can mix with the air more evenly to ensure a more complete combustion. A complete combustion will increase the fuel efficiency and reduce the emission of engine.

The governing equations for flows involving liquid/vapor phase transitions are

$$
\begin{aligned}
&\rho_t + \nabla\cdot(\rho\mathbf{u}) = 0,\\
&(\rho\mathbf{u})_t + \nabla\cdot(\rho(\mathbf{u}\mathbf{u}) + \mathbf{P}) = 0,\\
&(\lambda\rho)_t + \nabla\cdot(\lambda\rho\mathbf{u}) = \frac{w}{\gamma} + \nabla\cdot(\mu\rho\nabla\lambda),\\
&E_t + \nabla\cdot(\mathbf{u}E + \mathbf{u}\cdot\mathbf{P}) = \kappa\Delta T + L(T)\nabla\cdot(\mu\rho\nabla\lambda),\\
&\mathbf{P} = \left(p + \left(\frac{2}{3}\epsilon_1 - \epsilon_2\right)(\nabla\cdot\mathbf{u})\right) I - \epsilon_1(\nabla\mathbf{u} + \nabla\mathbf{u}^T),\\
&p_\rho > 0,\ p_{\rho\rho} > 0,\ p_\lambda > 0.
\end{aligned}
\tag{1.1}
$$

See [16]. The major symbols in the equations are as follows:

ρ	$\mathbf{u}$	λ	E	$\mathbf{P}$
density	velocity	mass fraction of vapor	energy density	stress-strain tensor

*Received by the editors January 24, 2011; accepted for publication (in revised form) October 10, 2011; published electronically February 14, 2012.
http://www.siam.org/journals/sima/44-1/82213.html

†Department of Mathematics, Georgetown University, Washington, DC 20057 (fan@math.georgetown.edu).
‡Department of Mathematics, North Carolina State University, Raleigh, NC 27695-8205 (xblin@math.ncsu.edu).

The constant μ is the diffusion coefficient of vapor, κ is the heat conduction coefficient, ϵ_1 and ϵ_2 are the coefficients of shear and bulk viscosities (cf. [3, 41]), and $L(T)$ is the latent heat.

The vapor production rate is w/γ, where γ is the typical reaction time and

$$w = (p - p_e)\lambda(\lambda - 1)\rho, \quad p < p_e. \tag{1.2}$$

The constant p_e is the equilibrium pressure. We consider only evaporation waves in this paper. Since $0 \le \lambda \le 1$, the assumption $p < p_e$ is to ensure $w \ge 0$.

Most liquid fuels are retrograde fluids that have sufficiently high molar specific heat capacity. This allows us to use the isothermal case of (1.1). Assume that the fuel is injected from the smaller end of the cone, and the cone's boundary is slippery, offering no resistance to tangential flows at the boundary. For the spherically symmetric flow, (1.1) reduces to the following system:

$$\begin{aligned} &\rho_t + (\rho u)_r + \frac{2\rho u}{r} = 0, \\ &(\rho u)_t + (\rho u^2 + p)_r + \frac{2\rho u^2}{r} = \epsilon \left(u_r + \frac{2u}{r} \right)_r, \\ &(\lambda\rho)_t + (\lambda\rho u)_r + \frac{2\lambda\rho u}{r} = \frac{1}{\gamma}(p - p_e)\lambda(\lambda - 1)\rho + \mu \left((\rho\lambda_r)_r + \frac{2\rho\lambda_r}{r} \right). \end{aligned} \tag{1.3}$$

If $\eta = \epsilon_2 - \frac{2}{3}\epsilon_1$ as in (1.1), then a straightforward but rather lengthy calculation shows that the combined viscosity ϵ in (1.3) is $\epsilon = \eta + \epsilon_1 = \frac{1}{3}\epsilon_1 + \epsilon_2$.

Because the typical reaction time γ, the diffusion coefficient of vapor μ, and the viscosity ϵ are all proportional to the mean free path, we shall assume that

$$\gamma = \epsilon/a, \quad \mu = \epsilon b.$$

To achieve a steady evaporation inside the nozzle, we look for the stationary solution of (1.3) which satisfies the following system:

$$\begin{aligned} &(\rho u)_r + \frac{2\rho u}{r} = 0, \\ &(\rho u^2 + p)_r + \frac{2\rho u^2}{r} = \epsilon \left(u_r + \frac{2u}{r} \right)_r, \\ &(\lambda\rho u)_r + \frac{2\lambda\rho u}{r} = \frac{a}{\epsilon}(p - p_e)\lambda(\lambda - 1)\rho + \epsilon b \left((\rho\lambda_r)_r + \frac{2\rho\lambda_r}{r} \right). \end{aligned} \tag{1.4}$$

The radius of the cone is in the range $r_1 \le r \le r_2$. Since ϵ is a small parameter, the system is singularly perturbed. We look for solutions of (1.4) with an internal layer at $r_0 \in (r_1, r_2)$. More specifically, there is an "intermediate variable" $\eta = \epsilon^\beta, 0 < \beta < 1$, such that the domain $[r_1, r_2]$ splits into three parts:

$$\begin{aligned} &[r_1, r_2] = I_1 \cup I_0 \cup I_2, \quad \text{where} \\ &\quad I_1 = [r_1, r_0 - \eta], I_0 = (r_0 - \eta, r_0 + \eta), I_2 = [r_0 + \eta, r_2]. \end{aligned} \tag{1.5}$$

The vapor fraction of the flow is $\lambda \approx 0$ in I_1 and $\lambda \approx 1$ in I_2, while a sudden change from $\lambda \approx 0$ to $\lambda \approx 1$ occurs in I_0. The interval I_0 is called the internal layer (or the fast, singular layer), while I_1 and I_2 are called the slow layers (or the regular, outer layers). We also call the solutions in $I_1 \cup I_2$ and I_0 slow (or regular) and fast (or internal) layers.

The intermediate variable satisfies the property $\eta \to 0$ as $\epsilon \to 0$, so in the singular limit I_0 becomes a point at r_0. Define the stretched variable (or the fast time) $\xi = (r - r_0)/\epsilon$. Let the internal layer I_0 in the stretched variable be denoted as

$$I_0(\xi) = (-\eta/\epsilon, \eta/\epsilon). \tag{1.6}$$

As $\epsilon \to 0, I_0(\xi) \to (-\infty, \infty)$. This allows us to consider the limits of the internal layer as $\xi \to \pm\infty$ in the asymptotic matching of internal and regular layers. The choice of intermediate variable is not unique. In some papers $\eta = \epsilon|\log(\epsilon)|$ was used.

We assume that the fluid moves along the radius direction, i.e., $u > 0$. In the following figure, the internal layer appears as a thin line at $r = r_0$:

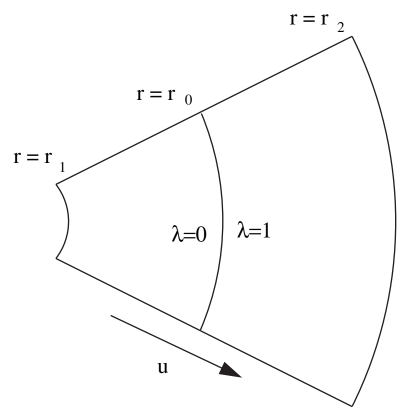

A brief review of relevant literature is in order. The validation of the model (1.1) was checked in [13] and [16] by comparing the phenomena observed in actual experiments in [12], [39], and [40] to the behavior of the one-dimensional isothermal case of (1.1) in Lagrange coordinate

$$\begin{aligned} v_t - u_x &= 0, \\ u_t + p(\lambda, v)_x &= \epsilon u_{xx}, \\ \lambda_t &= \frac{1}{\gamma} w(\lambda, v) + \beta \lambda_{xx}. \end{aligned} \tag{1.7}$$

The existence and nonexistence of phase-changing traveling waves of various types were shown in [13], [15], and [17] for the isothermal case. The proof of the existence of these traveling waves was much simplified by Fan and Lin in [18]. Fan and Corli [9] showed the existence and uniqueness of the solution of Riemann problem for inviscid (1.7) with $\epsilon = \gamma = \beta = 0$. Amadori and Corli established the existence of global solutions to the initial value problem of (1.7) for a class of initial data of large total variations. They also showed the convergence of solutions in the zero reaction time limit [1, 2]. Trivisa, in [41], proved the existence of variational solutions of the system (1.1) under various assumptions.

Although the spherically symmetric flow of (1.1) has not been studied before, previous research on spherical waves in gas dynamics can certainly shine light on the spherically symmetric solutions of (1.1) involving phase transitions. Slemrod [38] proved the existence of solutions of the spherically symmetric piston problem via vanishing similarity viscosity. Yang [44] studied the spherically symmetric Euler equations with initial data being small perturbations of a constant state and constructed the solutions by Glimm's scheme. Hsiao, Luo, and Yang [26] established the global existence of spherically symmetric banded variation (BV) solutions for the damped Euler system. Chen et al. [6] considered the spherically symmetric piston problem where they constructed a global entropy solution by using the shock capturing approach and the method of compensated compactness.

The spherically symmetric flow can be regarded as a special type of nozzle flow. The studies of nozzle flow were pioneered by Courant and Friedrichs [10] and Liu [32]. Many authors have studied the transonic flows in nozzles; see the recent articles [5, 7, 8, 29, 42, 43] and references cited therein. Hong, Hsu, and Liu [23, 24] and Liu and Oh [25] used the dynamical systems approach to study one-dimensional standing wave solutions of gas flows in a nozzle with variable cross-sectional area $a(x)$. When applied to the spherically symmetric nozzle, $a(x) = cx^2$, their system is approximately but not the same as the first two equations of our system (1.4). While all these papers studied the gas flow in a nozzle, we shall consider fluid flow in a nozzle with phase changes in this paper, using the dynamical systems approach.

The main contributions of this paper are as follows. We have characterized the conditions for the existence of the supersonic and subsonic standing waves. We have proved the existence of the internal layer for the limiting system with $\epsilon = 0$ in Theorems 4.2 and 4.3. We have shown that under suitable boundary conditions there exists a unique standing wave solution for small nonzero ϵ in Theorem 6.2 and Proposition 6.2. We have introduced a numerical method which is suitable for computing the internal layer solutions. We have also verified numerically that the heteroclinic orbit representing the internal layer is a transverse heteroclinic orbit in Theorem 5.1. The transversality condition is important to ensure the existence of a standing wave solution when ϵ is small and positive.

The outline of this paper is as follows. In section 2, we define the slow and fast times and recast the system into slow and fast systems. In section 3, we define the slow manifold and study the flow on the slow manifold. The most technical part of the paper is section 4, where we prove the existence of a heteroclinic solution for the fast system that connects pure liquid state $\lambda = 0$ to pure vapor state $\lambda = 1$. The heteroclinic solution is the singular limit of the internal layers as $\epsilon \to 0$. Sketches of the standing waves are given in Figures 3.2 and 4.2. In section 5, we present numerical simulation of the heteroclinic orbit proved in section 4. We introduce a multiple-step numerical shooting method which overcomes a technical problem in the numerical simulation. The numerical computation of the orbits also shows that the heteroclinic orbit is a transverse heteroclinic orbit; cf. Figures 5.5 and 5.6. In section 6 we present the main existence theorem of the standing waves when $\epsilon > 0$. The standing wave solution is near the union of three singular limit solutions, part of which is the two slow layers defined on $I_1 \cup I_2$ as in section 3, and part of which is an internal layer defined on I_0 as in section 4. The proof of Theorem 6.2 is based on the exchange lemma [22, 4, 36] from the geometric theory of singular perturbations and can also be proved by a functional analytic method as in [30, 21, 31]. We give only an outline of the proof in this paper.

2. Change of variables and definitions of the fast and slow systems. Since ϵ is a small parameter, we shall use the singular perturbation method to simplify the system. In the geometric singular perturbation theory, it is customary to convert (1.4) into an autonomous system. Let $s = r$ be an independent variable so that $dr/ds = 1$. Substituting into (1.4), the corresponding autonomous system in the slow time $s \in [r_1, r_2]$ is

$$
\begin{aligned}
&r_s = 1, \quad m_s = -\frac{2m}{r}, \\
(2.1) \qquad &(mu + p)_s + \frac{2mu}{r} = \epsilon \left(u_s + \frac{2u}{r} \right)_s, \\
&(m\lambda)_s + \frac{2m\lambda}{r} = \frac{a}{\epsilon}(p - p_e)\lambda(\lambda - 1)\rho + \epsilon b \left((\rho\lambda_s)_s + \frac{2\rho\lambda_s}{r} \right).
\end{aligned}
$$

A quick introduction to the singular perturbation method can be found in [33, 28]. Not only the domain $[r_1, r_2]$ splits into three regions: $I_1 \cup I_0 \cup I_1$; the unknown variables also split into slow variables and fast variables. When $\epsilon = 0$, such decomposition reduces the dimension of the system in both fast and slow layers.

The slow variables are those whose C^1 norms are bounded as $\epsilon \to 0$. Since both u and λ will have sudden jumps near $r_0 \in (r_1, r_2)$, they are not slow variables.

The original variables in the phase space with respect to the slow time s are $(\rho, u, \dot{u}, \lambda, \dot{\lambda})$. Define the new phase variables $(m, n, u, \lambda, \theta)$ as follows:

$$
\begin{aligned}
(2.2) \qquad &m := \rho u, \ n := \epsilon \dot{u} - \rho u^2 - p(\lambda, \rho), \\
&u = u, \ \lambda = \lambda, \ \theta := \epsilon b \rho \dot{\lambda}.
\end{aligned}
$$

At any $r_1 \leq \bar{s} \leq r_2$, let $\xi = (s - \bar{s})/\epsilon$ be the fast time. Any function f in slow time can be expressed in the fast time as $f(s) = f(\bar{s} + \epsilon\xi)$. Denote $\dot{f} = df/ds$ and $f' = df/d\xi$. Then

$$
n := u' - \rho u^2 - p(\lambda, \rho), \quad \theta := b\rho\lambda'.
$$

In this paper, we consider only the case $\rho, u > 0$ for all $s \in [r_1, r_2]$. Then the change of variables in (2.2) is invertible:

$$
\begin{aligned}
&u = u, \ \rho = m/u, \ \lambda = \lambda, \ \lambda' = \theta u/(bm), \\
&u' = n + mu + p(\lambda, m/u).
\end{aligned}
$$

The second equation of (2.1) can be integrated to yield $m(r) = M/r^2$, where M is an arbitrary constant. This reduces the number of variables by one. In the new phase space, (r, n) are the slow variables and (u, λ, θ) are the fast variables. Using the slow time s, the slow system in the new variables is

$$
\begin{aligned}
&\dot{r} = 1, \\
&\dot{n} = \frac{2mu}{r} - \left(\frac{2\epsilon u}{r} \right)_s, \\
(2.3) \qquad &\epsilon\dot{u} = n + mu + p(\lambda, m/u), \\
&\epsilon\dot{\lambda} = \frac{\theta u}{bm}, \\
&\epsilon\dot{\theta} = -aw + \frac{\theta u}{b} - \frac{2\epsilon\theta}{r},
\end{aligned}
$$

where w is defined in (1.2).

Using the fast time $\xi = (s - r_0)/\epsilon)$ the fast system in the new phase variables is

$$
\begin{aligned}
r' &= \epsilon,\\
n' &= \frac{2\epsilon mu}{r} - \left(\frac{2\epsilon u}{r}\right)_{\xi},\\
u' &= n + mu + p(\lambda, m/u),\\
\lambda' &= \frac{\theta u}{bm},\\
\theta' &= -aw + \frac{\theta u}{b} - \frac{2\epsilon\theta}{r}.
\end{aligned}
\tag{2.4}
$$

When the standing wave is in the outer layers $I_1 \cup I_2$, $(\dot{u}, \dot{\lambda}, \dot{\theta}) = O(1)$. Letting $\epsilon \to 0$ in (2.3), we have a systems of algebraic-differential equations in $I_1 \cup I_2$:

$$
\begin{aligned}
\dot{r} &= 1,\\
\dot{n} &= \frac{2mu}{r},\\
0 &= n + mu + p(\lambda, m/u),\\
0 &= \frac{\theta u}{bm},\\
0 &= -aw + \frac{\theta u}{b}.
\end{aligned}
\tag{2.5}
$$

The limit of (2.4), as $\epsilon \to 0$, satisfies

$$
\begin{aligned}
r' &= 0,\\
n' &= 0,\\
u' &= mu + p(\lambda, m/u) + n,\\
\lambda' &= \frac{\theta u}{bm},\\
\theta' &= -aw + \frac{\theta u}{b}.
\end{aligned}
\tag{2.6}
$$

(HH) Assume that there is a connected open set in (m, n, u) space such that for both $\lambda = 0$ and 1, the equation

$$n + mu + p(\lambda, m/u) = 0$$

can be uniquely solved by a smooth function $u = u^*(m, n, \lambda)$.

We now define a singular standing wave solution as the union of three functions defined on I_1, I_0, and I_2, respectively. Under the condition (HH), from the last three algebraic equations of (2.5) we can solve (λ, θ, u) as functions of (m, n):

$$\lambda = 0 \text{ or } 1,\ \theta = 0, u = u^*(m, n, \lambda).$$

Let $(r_1(s), n_1(s)), s \in [r_1, r_0]$ be a solution of the first two equations of (2.5), where $u = u^*(m, n, \lambda = 0)$. Let $\lambda_1(s) \equiv 0, \theta_1(s) \equiv 0,\ u_1(s) = u^*(m(s), n_1(s), \lambda = 0)$. Then $Y_1(s) := (\lambda_1, \theta_1, u_1, r_1, n_1)(s)$ is the part of the singular standing wave on I_1.

Let $(r_2(s), n_2(s)), s \in [r_0, r_2]$ be a solution of the first two equations of (2.5), where $u = u^*(m, n, \lambda = 1)$. Let $\lambda_2(s) \equiv 1, \theta_2(s) \equiv 0,\ u_2(s) = u^*(m(s), n_2(s), \lambda =$

1). Then $Y_2(s) := (\lambda_2, \theta_2, u_2, r_2, n_2)(s)$ is the part of the singular standing wave in I_2. The slow variables do not have jumps across r_0. Therefore we require that $n_1(r_0) = n_2(r_0),\ r_1(r_0) = r_2(r_0)$. Since $dr/ds = 1$, without loss of generality, let $r_1(s) = r_2(s) = s$.

Finally, from the first two equations of (2.6), the variables $(r, n) = (r_0, n_0)$ are constant in the fast time ξ. Let $(u_0(\xi), \lambda_0(\xi), \theta_0(\xi)), \xi \in (-\infty, \infty)$ be a heteroclinic solution of the last three equations of (2.6), connecting $(u_0(-\infty), \lambda_0(-\infty), \theta_0(-\infty)) = (u_-, \lambda_-, \theta_-)$ to $(u_0(\infty), \lambda_0(\infty), \theta_0(\infty)) = (u_+, \lambda_+, \theta_+)$. We assume that the asymptotic matching conditions are satisfied:

$$\begin{aligned} &u_- = u^*(m_0, n_0, \lambda = 0),\ u_+ = u^*(m_0, n_0, \lambda = 1),\\ &\lambda_- = 0,\ \lambda_+ = 1,\ \theta_\pm = 0. \end{aligned} \tag{2.7}$$

The function $Y_0(\xi) := (r_0, n_0, u_0, \lambda_0, \theta_0)(\xi)$ is the part of the singular standing wave on $I_0(\xi) = (-\infty, \infty)$; cf. (1.5) and (1.6).

DEFINITION 2.1. *The union of singular limit solutions Y_1, Y_0, and Y_2 on $I_1, I_0(\xi)$, and I_2 as defined above is called a singular standing wave solution.*

3. The limiting slow system and solutions on the slow manifolds.

3.1. The limiting slow system and the slow manifold. The solutions of the last three algebraic equations of (2.5) form a two-dimensional slow manifold. Since $u \neq 0$, we have $\theta = 0$ and $w = 0$. From $w = 0$ and $p < p_e$, we have $\lambda = 0$ or 1. The slow manifold has two disjoint components corresponding to $\lambda = 0$ and 1. Each of them will be called a slow manifold if no confusion should arise:

$$\begin{aligned} S_0 :=&\{\lambda = 0, \theta = 0, n + mu + p(0, m/u) = 0\},\\ S_1 :=&\{\lambda = 1, \theta = 0, n + mu + p(1, m/u) = 0\}. \end{aligned} \tag{3.1}$$

For $\lambda = 0$ or 1, the manifold can be expressed as

$$n = n(m, \lambda, u) := -mu - p(\lambda, m/u).$$

Using $p_\rho > 0,\ p_{\rho\rho} > 0$, we have

$$\begin{aligned} \frac{\partial n}{\partial u} &= -m + p_\rho \cdot \frac{m}{u^2},\\ \frac{\partial^2 n}{\partial u^2} &= -p_{\rho\rho}\left(\frac{m}{u^2}\right)^2 - 2p_\rho \frac{m}{u^3} < 0. \end{aligned}$$

Therefore, if $\bar{m} > 0, \lambda = 0, 1$ are fixed, as a function of u, $n(\bar{m}, \lambda, u)$ is concave downward. Define the $\bar{m}$ section of S_0 and S_1 as the following one-dimensional manifolds:

$$S_0(\bar{m}) := S_0 \cap \{m = \bar{m}\}, \quad S_1(\bar{m}) := S_1 \cap \{m = \bar{m}\}.$$

Due to $p_\rho > 0$ and $p_{\rho\rho} > 0$, when $u \to 0$, $n(m, \lambda, u) \to -\infty$. It is also obvious that when $u \to \infty$, $n(m, \lambda, u) \to -\infty$. Therefore for each (λ, m) there exists a maximum for $n(m, \lambda, u)$ that occurs at the point where $\partial n/\partial u = 0$. It is easy to see that at the maximum we have $u^2 - p_\rho = 0$. See Figure 3.1 for the graphs of a sequence of $S_0(m)$, where the pressure function is $p = 0.2 * \rho^2$.

Thus, in the (m, u, n) space the graphs of S_0 and S_1 are single humped folds, and each has a maximum on the m section $S_j(m)$, where $u^2 = p_\rho$.

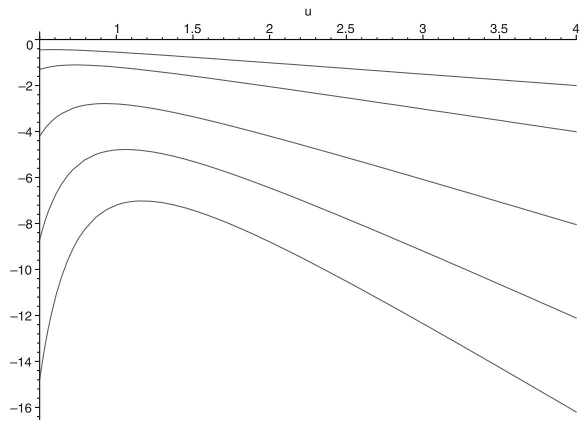

FIG. 3.1. *Cross-sectional view $S_0(m)$ of the slow manifold for the fixed $\lambda = 0$. From top to bottom are the graphics for $n = n(m, u)$ with $m = 0.5, 1, 2, 3, 4$.*

DEFINITION 3.1. *If $u^2 - p_\rho < 0$, then we say that the wave is subsonic. If $u^2 - p_\rho > 0$, then we say that the wave is supersonic. The surface where $u^2 - p_\rho = 0$ is called the sonic surface.*

Each slow manifold $S_j, j = 0, 1$ has two smooth branches separated by the sonic surface:

$$S_j^- = S_j \cap \{u^2 - p_\rho < 0\}, \quad S_j^+ = S_j \cap \{u^2 - p_\rho > 0\}.$$

If we specify whether it is on the supersonic or subsonic branch, then for $\lambda = 0, 1$, u can be expressed as functions of (r, n). The limiting slow manifolds become

$$\begin{aligned} S_j^- &:= \{\lambda = j, \theta = 0, u = u^-(m(r), n, \lambda = j)\}, \\ S_j^+ &:= \{\lambda = j, \theta = 0, u = u^+(m(r), n, \lambda = j)\}. \end{aligned} \tag{3.2}$$

On each two-dimensional manifold $S_j^\pm$ condition (HH) is satisfied. With the slow variables (r, n) as coordinates, the limiting slow system becomes

$$\begin{aligned} \dot{r} &= 1, \\ \dot{n} &= \frac{2mu^\pm(m(r), n, \lambda)}{r}, \quad \lambda = 0, 1. \end{aligned} \tag{3.3}$$

3.2. Solutions for the slow system. System (3.3) involves the function $u^\pm(m, n, \lambda)$ so it is not easy to get much qualitative information from it. Because the change of variables $n \leftrightarrow u$ is nonsingular on each branch $S_j^\pm, j = 0, 1$, we could use the variables (r, u) or (r, ρ) as coordinates on the slow manifold. Recall that $m := \rho u = Mr^{-2}$, where $M > 0$ is any given constant.

LEMMA 3.2. *On each supersonic or subsonic branch of the slow manifold, $S_0^\pm$ or $S_1^\pm$, defined as $\lambda = 0, 1,\ \theta = 0, u = u^\pm(m(r), n, \lambda)$, the equations for u, ρ are*

$$\begin{aligned} \frac{\dot{u}}{u}(u^2 - p_\rho(\lambda, m/u)) &= \frac{2p_\rho(\lambda, m/u)}{r}, \\ \rho\dot{\rho}(u^2 - p_\rho(\lambda, \rho)) &= \frac{-2m^2}{r}. \end{aligned}$$

In particular,

(1) *If* $u^2 > p_\rho$, *then* $\dot{u} > 0$, $\dot{\rho} < 0$;

(2) *If* $u^2 < p_\rho$, *then* $\dot{u} < 0$, $\dot{\rho} > 0$;

(3) $\dot{n} > 0$ *on both super and subsonic branches.*

Proof. It is easy to derive (3) from (3.3) directly.

From the first equation of (1.4), we have

$$u(\rho u)_r + \frac{2\rho u^2}{r} = 0.$$

Subtracting this from the second equation and letting $\epsilon = 0$ and $r = s$, we have

$$m\dot{u} + \dot{p} = 0. \tag{3.4}$$

Since $\dot{\lambda} = 0$ if $\lambda = 0, 1$, we have $p_s = p_\rho \dot{\rho}$. From (3.4), we have

$$mu\dot{u} + p_\rho u\dot{\rho} = mu\dot{u} + u\dot{p} = 0. \tag{3.5}$$

From the first equation of (1.4) again, we have

$$u\dot{\rho} + \rho\dot{u} = \frac{-2m}{r}. \tag{3.6}$$

Combining (3.5) and (3.6), we obtain an equation for $u(s)$:

$$\begin{aligned} mu\dot{u} - p_\rho(\rho\dot{u} + 2m/r) &= 0, \\ u\dot{u} - p_\rho\rho\dot{u}/m - 2p_\rho/r &= 0. \end{aligned}$$

$$\frac{\dot{u}}{u}(u^2 - p_\rho) = \frac{2p_\rho}{r}. \tag{3.7}$$

From (3.6), we have

$$m\rho\dot{u} = -\frac{2m^2}{r} - mu\dot{\rho}.$$

Combining the above with (3.4), we obtain an equation for $\rho(s)$:

$$\begin{aligned} m\rho\dot{u} + \rho p_\rho\dot{\rho} &= 0, \\ \left(\frac{-2m^2}{r} - mu\dot{\rho}\right) + \rho p_\rho\dot{\rho} &= 0. \end{aligned}$$

$$\rho\dot{\rho}(u^2 - p_\rho) = \frac{-2m^2}{r}. \tag{3.8}$$

Equations (3.7) and (3.8) are precisely the first two equations in this lemma. Inequalities (1) and (2) of the lemma then follow easily. ∎

THEOREM 3.3. *For* $\lambda = 0$ *or* 1, *each of the two branches of the slow manifold is invariant under the slow flow. In particular, the sonic surface cannot be reached by the reduced flow on the slow manifold in forward time.*

Proof. Let $d = u^2 - p_\rho$, which measures the signed distance to the transonic surface. Then $d < 0$ or $d > 0$ on the subsonic or supersonic branch of $S_0^\pm$ and $S_1^\pm$. Using Lemma 3.2, we have

$$\begin{aligned} \dot{d} &= 2u \cdot \dot{u} - p_{\rho\rho} \cdot \dot{\rho} \\ &= \frac{4u^2 p_\rho}{rd} + \frac{2m^2 p_{\rho\rho}}{rd\rho}. \end{aligned} \tag{3.9}$$

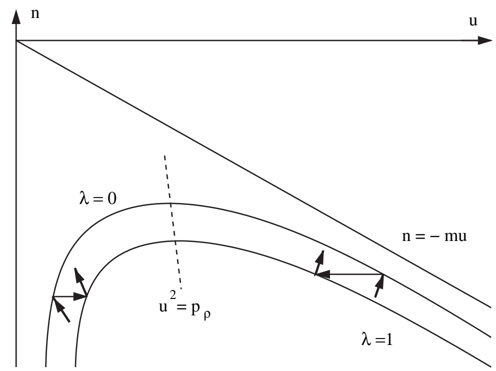

FIG. 3.2. *Since $p_\lambda > 0$ the manifold S_0 is strictly above S_1. Subsonic and supersonic internal layers connecting $\lambda = 0$ to $\lambda = 1$ are depicted as two thin arrows. The slow layers defined on $I_1 \cup I_2$ are plotted as thick arrows on the slow manifold. The dotted line is the sonic surface.*

From this we have

$$\frac{d}{ds}(d^2) = \frac{8u^2 p_\rho}{r} + \frac{4m^2 p_{\rho\rho}}{r\rho} > 0.$$

Thus, d^2 increases only in forward time, i.e., if $d > 0$, then $\dot{d} > 0$, and if $d < 0$, then $\dot{d} < 0$. This proves the theorem. ∎

The sonic surface intersects with $\lambda = 0$ and $\lambda = 1$ in two lines. Based on Theorem 3.3, the lines are unstable with respect to the flows on the slow manifolds.

From Lemma 3.2, $\dot{u} > 0$ on the supersonic branches and $\dot{u} < 0$ on the subsonic branches; also $\dot{n} > 0$ for both super and subsonic flows. These informations give a good description of the variables (u, n) in slow layers.

In Figure 3.2, for a fixed m, cross sections of the slow manifolds $S_0(m)$ and $S_1(m)$ are plotted. If $m = m_0$, the internal layer solutions defined on I_0 may exist and are plotted as thin horizontal arrows where (m, n, r) are fixed. The direction of the arrow, i.e., the signs of u', will be discussed in the next section. The slow layers defined on $I_1 \cup I_2$, are plotted as thick arrows. They are not on the curve $S_0(m_0)$ or $S_1(m_0)$, because the m components of the solutions are not constant on $I_1 \cup I_2$.

In Figure 3.1 several curves $S_j(m)$ corresponding to several m are plotted. As time s increases, the $m(s)$ value decreases so the solution should move from curves with lower n to greater n. Notice that the direction of change of u with respect to s agrees with Figure 4.2 in the next section.

3.3. Boundary and initial value problems for the slow system. We shall restrict ourselves to either the super or the subsonic case. Let $n_1(s), n_2(s), r_1 \le s \le r_2$ be the solution of the following equations:

$$\dot{n}_1 = \frac{2mu^\pm(m, n_1, (\lambda = 0))}{r}, \tag{3.10}$$

$$\dot{n}_2 = \frac{2mu^\pm(m, n_2, (\lambda = 1))}{r}. \tag{3.11}$$

LEMMA 3.4. *If the orbits of* (3.10) *and* (3.11) *meet at* (r_0, n_0)*, then* $(d/ds)n_1(r_0) \ne (d/ds)n_2(r_0)$*, i.e., the intersection is transversal in the* (r, n) *plane.*

Proof. Prove by contradiction. If the curves meet tangentially, then

$$(d/ds)n_1(r_0) = (d/ds)n_2(r_0).$$

From the differential equations for $n_1(r)$ and $n_2(r)$ and the fact $m(r)$ is a continuous function, $m(r_0-) = m(r_0+)$, we have $u^{\pm}(m(r_0), n(r_0), 0) = u^{\pm}(m(r_0), n(r_0), 1)$. Therefore $\rho(r_0-) = \rho(r_0+)$. Using $\partial p/\partial\lambda > 0$, we would have $p(\lambda = 0, \rho_-) < p(\lambda = 1, \rho_+)$. Let $(u_\pm, n_\pm, m_\pm, p_\pm)$ be the values of (u, n, m, p) on S_1 and S_0, respectively. Then from $u_- = u_+, n_- = n_+, m_- = m_+$, and

$$n = -mu - p(\lambda, m/u), \tag{3.12}$$

we have $p_- = p_+$, contradicting to $p(\lambda = 0, \rho_-) < p(\lambda = 1, \rho_+)$. □

Remark 3.1. Based on Lemma 4.1 in the next section, if an internal layer solution can exist at the intersection point r_0, we must have $u_- < u_+$ for a subsonic internal layer and $u_- > u_+$ for a supersonic internal layer. Therefore, at the point $r = r_0$, we have

$$\begin{aligned} &(d/ds)n_1(r_0) < (d/ds)n_2(r_0) \quad \text{for a subsonic internal layer,} \\ &(d/ds)n_1(r_0) > (d/ds)n_2(r_0) \quad \text{for a supersonic internal layer.} \end{aligned}$$

We now look for conditions on (r_0, m_0, n_0) so that there exists a piecewise smooth function

$$n(s) = \begin{cases} n_1(s), s \in [r_1, r_0], \\ n_2(s), s \in [r_0, r_2], \end{cases}$$

where n_1 and n_2 satisfy (3.10) and (3.11) with $n_1(r_0) = n_2(r_0) = n_0$. Defined on $I_j, j = 1, 2$, $n_j(s)$ shall be used to construct the outer layers of the singular standing wave.

Let r_0 be the position of the internal layer with $r_1 < r_0 < r_2$. From $m_0 = Mr_0^{-2}$, we can calculate M and hence $m(s) = Ms^{-2}$ for all s. We assume that $n_0 < 0$ satisfies the following condition:

$$n_0 < \max_{u>0} n(m_0, \lambda = 1, u). \tag{3.13}$$

Since $\max_{u>0} n(m_0, \lambda = 1, u) < \max_{u>0} n(m_0, \lambda = 0, u)$, condition (3.13) guarantees (m_0, n_0) is in the domain of $u^{\pm}(m_0, n_0, \lambda = 0)$ and $u^{\pm}(m_0, n_0, \lambda = 1)$. We need that condition to obtain two points on the slow manifolds S_0 and S_1 that have the same (m_0, n_0) coordinates and can stay on the same side of the sonic surface, either supersonic or subsonic. In the future the two points shall be connected by the internal layer illustrated as the thin arrow in Figure 3.2. With n_0 determined, we define

$$\begin{aligned} &u_1(r_0) = u^{\pm}(m_0, n_0, \lambda = 0), \ u_2(r_0) = u^{\pm}(m_0, n_0, \lambda = 1), \\ &\rho_1(r_0) = m_0/u_1(r_0), \ \rho_2(r_0) = m_0/u_2(r_0). \end{aligned}$$

Then with $(u_j(r_0), \rho_j(r_0))$ as initial conditions, we can calculate $(u_j(s), \rho_j(s)), j = 1, 2$, from Lemma 3.2, at least for a short time $s > 0$ for $(u_2(s), \rho_2(s))$ and $s < 0$ for $(u_1(s), \rho_1(s))$.

For s not small, it turns out that there is no need to impose any condition on $n_2(s)$ since Theorem 3.3 guarantees the solution will stay on the same side of the sonic surface in forward time starting from $s = r_0$. The next lemma ensures that if $r_0 - r_1$ is relatively small, and $|u^2 - p_\rho|$ is sufficiently large, then the backward solution $n_1(s), r_1 \le s \le r_0$, will also stay on the same side of the sonic surface.

LEMMA 3.5. *For the backward solution $n_1(s)$ starting from $n_1(r_0) = n_0$, assume that $d(r_0)$ is sufficiently large and $r_0 - r_1$ is sufficiently small such that the following integral for $r_1 < r_0$ is positive:*

$$d^2(r_0) + \int_{r_0}^{r_1} \left(\frac{8u^2 p_\rho}{r} + \frac{4m^2 p_{\rho\rho}}{r\rho} \right) ds > 0. \tag{3.14}$$

Here all the functions involved in the integral are the solutions of the slow system. Then the solution $n_1(s)$ will stay on the same side of the sonic surface for all $r_1 \le s \le r_0$. The condition (3.14) is also necessary.

Proof. If the condition (3.14) is satisfied, then for all $r \in [r_1, r_0]$,

$$d^2(r) = d^2(r_0) + \int_{r_0}^{r} \left(\frac{8u^2 p_\rho}{r} + \frac{4m^2 p_{\rho\rho}}{r\rho} \right) ds$$

will be positive and smaller than $d^2(r_0)$ So the solution $n_1(s)$ will stay on the same side of the slow manifold for all $r \in [r_1, r_0]$. ☐

4. Internal layer solutions for the fast system. To analyze the fast change of dynamics where the derivatives of some variables are of $O(1/\epsilon)$, the fast time $\xi = (s - r_0)/\epsilon$ shall be used for s near r_0. The limiting system of (2.4), as $\epsilon \to 0+$, satisfies (2.6).

From the first two equations of (2.6), $(r, n) = (r_0, n_0)$ are constants for all $\xi \in \mathbb{R}$. With $m = m_0 = m(r_0)$ and $n = n_0$ as two parameters, we look for a heteroclinic solution $(u, \lambda, \theta)(\xi)$ of the last three equations of (2.6). Assume the heteroclinic orbit connects

$$E_- := (u_-, \lambda_-, \theta_-) \text{ to } E_+ := (u_+, \lambda_+, \theta_+), \text{ as } \xi \to \mp\infty,$$

where $\lambda_- = 0, \lambda_+ = 1$, and $\theta_\pm = 0$. The entire slow manifolds S_0 and S_1 defined in (3.1) consist of equilibrium points for the last three equations of (2.6). Let the pressure at E_- and E_+ be p_- and p_+. From (3.12), we have

$$n = -mu_- - p_-.$$

Thus

$$u' = m(u - u_-) + (p - p_-).$$

System (2.6) becomes

$$\begin{aligned} \lambda' &= \frac{\theta u}{bm}, \\ \theta' &= -aw + \frac{\theta u}{b}, \\ u' &= m(u - u_-) + (p - p_-). \end{aligned} \tag{4.1}$$

Let $v := 1/\rho$. Define

$$\begin{gathered} \bar{p}(\lambda, v) := p(\lambda, 1/v) = p(\lambda, \rho), \\ \text{then } \partial\bar{p}/\partial v = -\rho^2 \partial p/\partial\rho. \end{gathered}$$

Since $p_\rho > 0$, we have $\bar{p}_v < 0$.

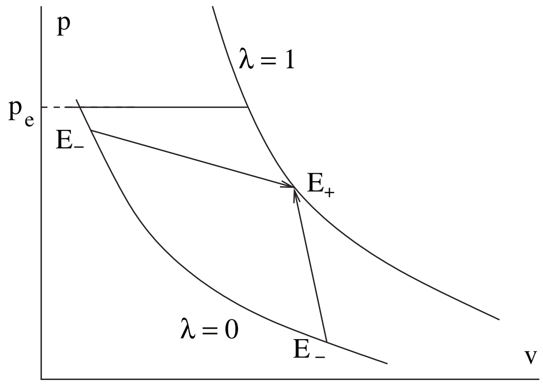

FIG. 4.1. *Two ways to connect E_- on $\lambda = 0$ to E_+ on $\lambda = 1$ by a line segment of negative slope. Note that $v = u/m$.*

Let $P^m(\lambda, u) := p(\lambda, \rho) = p(\lambda, m/u)$. Then

$$\partial P^m(\lambda, u)/\partial\lambda = p_\lambda(\lambda, \rho) > 0,$$
$$\partial P^m(\lambda, u)/\partial u = p_\rho \cdot \left(-\frac{m}{u^2}\right) < 0.$$

Using $\rho = m/u$, we obtain the following obvious result:

$$m^2 + \bar{p}_v = \frac{m^2}{u^2}(u^2 - p_\rho) = m(m + P_u^m). \tag{4.2}$$

Letting $\xi \to \infty$ in the last equation of (4.1), we have

$$m = -\frac{p_+ - p_-}{u_+ - u_-}.$$

Since $m > 0$, the slope of the line $\overline{E_- E_+}$ on the (u, p) plane is always negative. At the jump point r_0, we have

$$m(r_0) = -\frac{\bar{p}(1, v_+) - \bar{p}(0, v_-)}{m(r_0)/\rho_+ - m(r_0)/\rho_-},$$
$$m(r_0)^2 = -\frac{\bar{p}(1, v_+) - \bar{p}(0, v_-)}{v_+ - v_-}.$$

Based on the last equation, in the (v, p) plane, the slope of the line segment connecting $E_- = (v_-, p_-)$ and $E_+ = (v_+, p_+)$ is always negative. As seen in Figure 4.1, there are two possibilities: (1) The slope of $\overline{E_- E_+}$, in absolute value, is smaller than that of the tangent line at E_+. (2) The slope of $\overline{E_- E_+}$, in absolute value, is larger than that of the tangent line at E_+.

Since the slope of the line $\overline{E_- E_+}$ is $-m^2(r_0)$, it is also clear from Figure 4.1 that the standing waves satisfy the following lemma.

LEMMA 4.1. (1) *If $u^2 > p_\rho$ at $E_\pm$, then $m^2 + \bar{p}_v > 0$ at $E_\pm$. In this case we have*

$$\lambda_- = 0, \quad \lambda_+ = 1,$$
$$v_- > v_+, \quad u_- > u_+, \quad p_- < p_+.$$

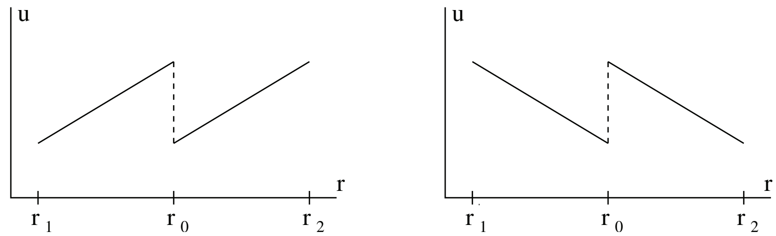

FIG. 4.2. *Sketch of the standing wave solutions in* (u, r) *coordinates. Left: supersonic; Right: subsonic.*

(2) *If* $u^2 < p_\rho$ *at* $E_\pm$*, then* $m^2 + \bar{p}_v < 0$ *at* $E_\pm$*. In this case we have*

$$\lambda_- = 0, \quad \lambda_+ = 1,$$
$$v_- < v_+, \quad u_- < u_+, \quad p_- > p_+.$$

The results of Lemma 4.1 agree with that in Figure 3.2. See also the following sketch of u as functions of r in Figure 4.2.

Note that for the subsonic flow, $m + P^m_u < 0$ if $u_- < u < u_+$. For the supersonic flow, $m + P^m_u > 0$ if $u_+ < u < u_-$. Based on this we can prove that for each fixed u between u_- and u_+, for both super- and subsonic flows, $m(u - u_-) + (p - p_-) < 0$ if $\lambda = 0$, and $m(u - u_-) + (p - p_-) > 0$ if $\lambda = 1$. Since $\partial P^m/\partial\lambda > 0$, there exists a unique $0 < \lambda < 1$ that solves the equation $m(u - u_-) + (p(\lambda, m/u) - p_-) = 0$. The solutions of this equation form a smooth curve $\mathcal{C}$ in the (u, λ) plane and can be expressed by a smooth function

$$\mathcal{C} := \{(u, \lambda) : \lambda = \lambda^c(u). \tag{4.3}$$

It will be called the isocline for u on which $u'(\xi) = 0$. If $m + P^m_u < 0$ (or > 0) then $d\lambda^c(u)/du > 0$ (or < 0).

From $w = (p - p_e)\lambda(\lambda - 1)\rho = (p - p_e)\lambda(\lambda - 1)mu^{-1}$, at $\lambda = 0$ or 1, we have

$$w_\lambda = (p - p_e)(2\lambda - 1)mu^{-1},$$
$$w_u = 0.$$

The linear variational system of (4.1) at $\lambda = 0, 1,\ \theta = 0$ is

$$\begin{pmatrix} \Lambda \\ \Theta \\ U \end{pmatrix}' = A \begin{pmatrix} \Lambda \\ \Theta \\ U \end{pmatrix}, \text{ where } A = \begin{pmatrix} 0 & u/(bm) & 0 \\ -aw_\lambda & u/b & 0 \\ P^m_\lambda & 0 & P^m_u + m \end{pmatrix}.$$

Consider the eigenvalue problem at $\lambda = 0, 1,\ \theta = 0$:

$$\det(kI - A) = \det \begin{pmatrix} k & -u/(bm) & 0 \\ aw_\lambda & k - u/b & 0 \\ -P^m_\lambda & 0 & k - P^m_u - m \end{pmatrix} = 0,$$
$$\left(k^2 - \frac{ku}{b} + \frac{a}{b}(p - p_e)(2\lambda - 1)\right)(k - P^m_u - m) = 0,$$
$$k_{1,2} = \frac{u}{2b} \mp \sqrt{\left(\frac{u}{2b}\right)^2 + \frac{a}{b}(p_e - p)(2\lambda - 1)},$$
$$k_3 = P^m_u + m = \frac{m}{u^2}(u^2 - p_\rho).$$

TABLE 1
The signs of eigenvalues and eigenvectors.

	E_-	E_+
subsonic case $u^2 < p_\rho$	$k_3 < 0$ $0 < k_1 < k_2$ $\Theta_1 > 0, \Theta_2 > 0$ $U_1 > 0, U_2 > 0$	$k_3 < 0$ $k_1 < 0 < k_2$ $\Theta_1 < 0 < \Theta_2$ $U_2 > 0, U_1$ varies
supersonic case $u^2 > p_\rho$	$k_3 > 0$ $0 < k_1 < k_2$ $\Theta_1 > 0, \Theta_2 > 0$ U_1, U_2 may vary	$k_3 > 0$ $k_1 < 0 < k_2$ $\Theta_1 < 0 < \Theta_2$ $U_1 < 0, U_2$ varies

Assume that
(C1) $p < p_e$ at both E_- and E_+;
(C2) $u^2 - 4ab(p_e - p) > 0$ at E_-.
Let the eigenvectors corresponding to k_j be $(\Lambda_j, \Theta_j, U_j)$.

Although not required, we assume $k_j \neq k_3, j = 1, 2$, so the eigenvectors corresponding to $k_j, j = 1, 2$, have simple expressions. Otherwise the generalized eigenvector may have to be used to express the eigenvectors, but the rest of the proof stays the same. The corresponding eigenvectors for k_j are

$$V_j := (\Lambda_j, \Theta_j, U_j) = \left(1, \frac{bm}{u}k_j, \frac{P^m_\lambda}{k_j - k_3}\right), \quad j = 1, 2, \tag{4.4}$$
$$V_3 := (\Lambda_3, \Theta_3, U_3) = (0, 0, 1),$$

The signs of $k_j, \Lambda_j, \Theta_j, U_j$ are summarized in Table 1.

Let R be the rectangular region such that

$$\begin{aligned} R :=& \{(\lambda, u) : 0 \le \lambda \le 1, u_- \le u \le u_+\} \quad \text{if } u- < u_+, \\ R :=& \{(\lambda, u) : 0 \le \lambda \le 1, u_+ \le u \le u_-\} \quad \text{if } u_+ < u_-. \end{aligned} \tag{4.5}$$

4.1. Supersonic internal layer. The main result of this subsection is the following theorem.

THEOREM 4.2. *For the existence of supersonic waves, we assume that*
(H1) $p < p_e$ *at* E_+ *and*
(H2) $u^2 - 4ab(p_e - p) > 0$ *for* $\{(\lambda, u) : \lambda = 0,\ u_+ < u < u_-\}$.
Then there exists a unique heteroclinic solution, up to a phase shift, (λ, θ, u) *connecting* E_- *to* E_+. *Moreover, the heteroclinic solution is monotone in the sense that* $d\lambda/d\xi > 0$ *and* $du/d\xi < 0$ *for all* $\xi \in \mathbb{R}$.

The rest of the subsection is devoted to proving Theorem 4.2.

The equi-pressure equation $P^m(\lambda, u) = p_e$ can be solved by

$$\lambda = \lambda_e(u), \quad \frac{d\lambda_e}{du} = -\frac{P^m_u}{P^m_\lambda} > 0. \tag{4.6}$$

From (H1) $p < p_e$ at $E_+ := \{\lambda = 1, \theta = 0, u = u_+\}$. Since $u \ge u_+$ in R (see (4.5)), from $\partial P^m/\partial u < 0$, we have $p < p_e$ in the entire region $(\lambda, u) \in R$. In particular for any $(\lambda, u) \in R$ and $\theta = 0$, we have $w > 0$ and $\theta' < 0$.

The eigenvalues at $E_- = \{\lambda = 0, \theta = 0, u = u_-\}$, under the conditions (H1) and (H2), satisfy

$$0 < k_1 < k_2,\ k_3 > 0.$$

The equilibrium E_- is unstable with $\dim W^u(E_-) = 3$.

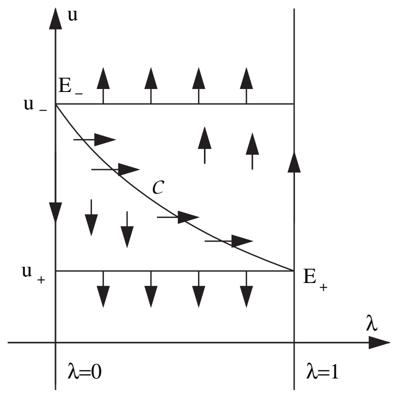

FIG. 4.3. *Vector field in the region R with $\theta > 0$.*

The eigenvalues at $E_+ = \{\lambda = 1, \theta = 0, u = u_+\}$ satisfy

$$k_1 < 0 < k_2, \; k_3 > 0.$$

The equilibrium E_+ is a saddle with $\dim W^u(E_+) = 2, \; \dim W^s(E_+) = 1$. The stable eigenvector corresponding to $k_1 < 0$ is

$$(\Lambda_1, \Theta_1, U_1) = \left(1, \frac{bm}{u} k_1, \frac{P_\lambda^m}{k_1 - k_3}\right)$$

with $\Lambda_1 > 0, \; \Theta_1 < 0, \; U_1 < 0$. We found that the projection of a branch of the local stable manifold $W^s(E_+)$ onto the (λ, u) plane enters the region R (cf. Figure 4.3). Extending the local stable manifold $W^s_{loc}(E_+)$ backward, we want to show it is connected to $W^u_{loc}(E_-)$.

Consider a pentahedron-shaped solid W in the (λ, θ, u) space bounded by the following surfaces:

$$\begin{aligned}
\text{Right side } \mathcal{F}_r &:= \{\lambda = 1, \; \theta > 0, \; u_+ < u < u_-\};\\
\text{Bottom side } \mathcal{F}_b &:= \{\theta = 0, \; 0 < \lambda < 1, \; u_+ < u < u_-\};\\
\text{Back side } \mathcal{F}_k &:= \{u_+ < u < u_-, \; \lambda = \lambda^c(u), \; \theta > 0\};\\
\text{Front side } \mathcal{F}_f &:= \{u = u^+, \; 0 < \lambda < 1, \; \theta > 0\};\\
\text{Slant side } \mathcal{F}_s &:= \{\theta - (m\lambda)/2 = 0, \; 0 < \lambda < 1, u_+ < u < u_-\}.
\end{aligned}$$

See (4.3) for the definition of $\lambda^c(u)$. In describing the surfaces of the solid W, we assume that the orientation of the axes are as follows. The λ–axis points to the right, the θ–axis points upward, and the u–axis points away from the viewer.

The outward normal of the slant side $\mathcal{F}_s$ is

$$\mathbf{n} = (-m/2, 1, 0).$$

The vector field on the slant side is

$$\mathbf{f} = ((\theta u)/(bm), -aw + (\theta u)/b, m(u - u_-) + (p - p_-)).$$

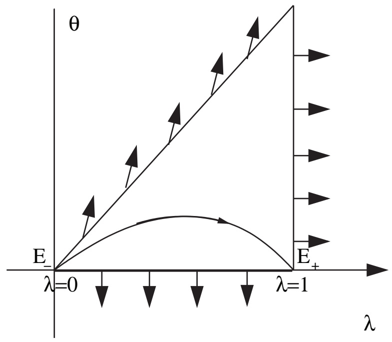

FIG. 4.4. *The flow leaves the pentahedron shaped solid W from all its surfaces.*

Therefore,

$$\begin{aligned}\mathbf{f}\cdot\mathbf{n} &= \frac{\theta u}{2b} - aw \\ &= \frac{m\lambda u}{4b} - a(p_e-p)\lambda(1-\lambda)m/u \\ &\geq \frac{m\lambda}{bu}\left(\frac{u^2}{4} - ab(p_e-p)\right) > 0.\end{aligned}$$

The last inequality is due to (H2), from which $\frac{u^2}{4} > ab(p_e-p)$ is valid for $\lambda = 0$ and $u_+ < u < u_-$. Thus is also valid if $\lambda > 0$ since for the same u, the pressure p is even greater. Thus the flow on $\mathcal{F}_s$ must leave W.

Since $d\lambda/d\xi = (u\theta)/(bm) > 0$, the flow on $\mathcal{F}_r$ must leave W.

Since $d\theta/d\xi = -ab(p_e-p)\lambda(1-\lambda)m/u < 0$, the flow on the bottom side $\mathcal{F}_b$ must leave W.

On the front side $\mathcal{F}_f$, if $\lambda = 1$, then $du/d\xi = m(u-u_+) + (p-p_+) = 0$. If $\lambda < 1$, due to $P^m_\lambda > 0$, we have $du/d\xi < 0$. The flow on $\mathcal{F}_f$ must leave W.

On the back side $\mathcal{F}_k$, the outward normal is $\mathbf{n} = (1, 0, -d\lambda^c/du)$. The vector field satisfies $\lambda' > 0,\ u' = 0$. Therefore $\mathbf{f}\cdot\mathbf{n} > 0$. The flow on $\mathcal{F}_k$ must leave W.

The results are summarized in Figure 4.4. It is also straightforward to check that the flow cannot enter W through the six edges of W.

We now pick a point P on $W^s_{loc}(E_+)$ in the interior of R with $\theta > 0$. It is easily verified that if $P \in W^s_{loc}(E_+)$ and is sufficiently close to E_+, then $P \in W$ due to the fact that $u'(\xi) < 0$ on the tangent space of $W^s_{loc}(E_+)$. The backward trajectory $\Phi(\xi, P) = (\lambda(\xi), \theta(\xi), u(\xi)), \xi \leq 0$, cannot leave W through all its surfaces and edges. Clearly $d\lambda/d\xi > 0$ and $du/d\xi < 0$ in W. Therefore, as $\xi \to -\infty$, being two bounded and monotone functions, the limits of $\lambda(\xi)$ and $u(\xi)$ exist. Based on this, it is easy to show that $\theta(\xi) \to 0$ as $\xi \to -\infty$. The alpha limit set $\alpha(P)$ must be the equilibrium point E_- on the boundary of W. The proof above also shows that the λ and u components of the heteroclinic solution are monotone.

4.2. Subsonic internal layer. The main result of this subsection is the following theorem.

THEOREM 4.3. *For the existence of subsonic waves, we assume*

(H1) $p < p_e$ *at the equilibrium point* E_- *and*

(H2) $u^2 - 4ab(p_e - p) > 0$ *on the isocline* $\mathcal{C}$ *where* $u' = 0$.

Then there exists a heteroclinic solution (λ, θ, u) *connecting* E_- *to* E_+*. Moreover, the heteroclinic solution is monotone in the sense that* $d\lambda/d\xi > 0$ *and* $du/d\xi > 0$ *for all* $\xi \in \mathbb{R}$.

The rest of this subsection is devoted to proving Theorem 4.3.

Recall the equation for the equi-pressure line $\lambda = \lambda_e(u)$ in (4.6) and the rectangular region R defined in (4.5). There are two possibilities:

(1) The entire rectangle R is in the region $p < p_e$.

(2) The rectangle R is divided by the line $\lambda = \lambda_e(u)$ into two parts.

In the second case, the isocline $\mathcal{C}$ and the equi-pressure line $\lambda = \lambda_e(u)$ do not intersect, as shown in the following lemma.

LEMMA 4.4. *Under the condition* (H1), *if the equi-pressure line* $\lambda = \lambda_e(u)$ *intersects the region* R *and divides* R *into two parts, then the entire isocline* $\mathcal{C}$ *for the* u*-equation is in the region* $p < p_e$*. The equi-pressure line* $\lambda = \lambda_e(u)$ *is in the region* $u' > 0$.

Proof. For $(\lambda, u) \in R \cap \{p = p_e\}$, since $p = p_e$ and condition (H1), we have $p > p_-$. Also observe that $u > u_-$ in R. Therefore $u' = m(u - u_-) + (p - p_-) > 0$ on the equi-pressure line $p = p_e$ in R. This proves the second statement of the lemma.

Since the two lines do not intersect, our assumption on one end of the isocline $\mathcal{C}$ implies that E_- is on the part of R where $p < p_e$. Therefore the entire isocline $\mathcal{C}$ is on the part of R where $p < p_e$. ∎

If $\lambda = 0, \theta = 0$, then under the condition (H2),

$$0 < k_1 < k_2,\ k_3 < 0.$$

The equilibrium E_- is a saddle with $\dim W^u = 2$.

If $\lambda = 1, \theta = 0$, then

$$k_1 < 0 < k_2,\ k_3 < 0.$$

The equilibrium E_+ is a saddle with $\dim W^s = 2$. The eigenvector at E_- corresponding to k_1 is

$$(\Lambda_1, \Theta_1, U_1) = \left(1, \frac{bm}{u} k_1, \frac{P_\lambda^m}{k_1 - k_3}\right) \text{ if } k_1 \neq k_3.$$

The eigenvector corresponding to k_3 is

$$(\Lambda_3, \theta_3, U_3) = (0, 0, 1).$$

Consider a pentahedron-shaped solid W in the (λ, θ, u) space bounded by the following surfaces:

$$\begin{aligned}
\text{Right side } \mathcal{F}_r &:= \{\lambda = 1,\ \theta > 0,\ u_- < u < u_+\};\\
\text{Bottom side } \mathcal{F}_b &:= \{\theta = 0,\ 0 < \lambda < 1,\ u_- < u < u_+\};\\
\text{Back side } \mathcal{F}_k &:= \{u_- < u < u_+,\ \lambda = \lambda^c(u),\ \theta > 0\};\\
\text{Front side } \mathcal{F}_f &:= \{u = u_-,\ 0 < \lambda < 1,\ \theta > 0\};\\
\text{Slant side } \mathcal{F}_s &:= \{\theta - (m\lambda)/2 = 0,\ u_- < u < u_+, \lambda^c(u) < \lambda < 1\}.
\end{aligned}$$

The definition of $\lambda^c(u)$ is in (4.3). See Figure 4.5 for the top view and front view of W.

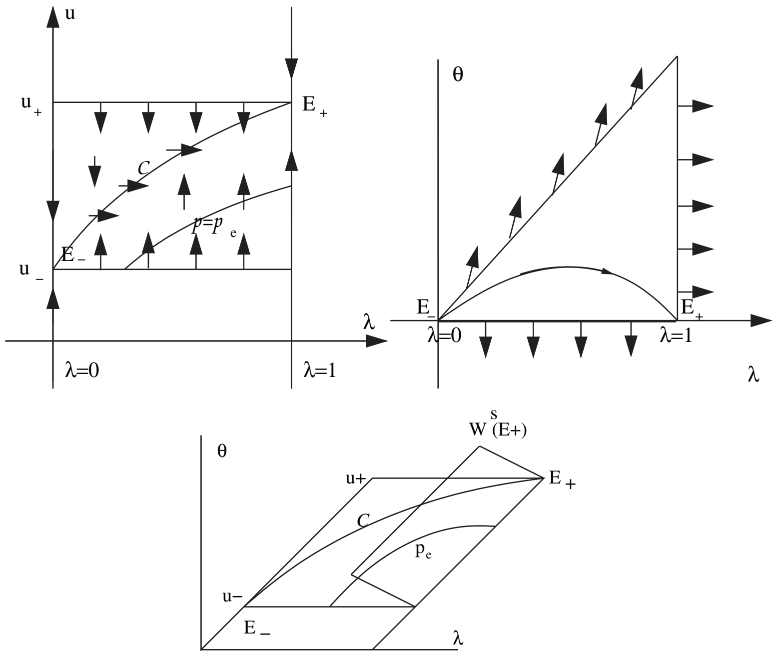

FIG. 4.5. *Vector field in the region R with $\theta > 0$.*

The outward normal of the slant side $\mathcal{F}_s$ is

$$\mathbf{n} = (-m/2, 1, 0).$$

The vector field on the slant side is

$$\mathbf{f} = ((\theta u)/(bm), -aw + (\theta u)/b, m(u - u_-) + (p - p_-)).$$

Therefore,

$$\begin{aligned} \mathbf{f} \cdot \mathbf{n} &= \frac{\theta u}{2b} - aw \\ &= \frac{m\lambda u}{4b} - a(p_e - p)\lambda(1-\lambda)m/u \\ &\geq \frac{m\lambda}{bu}\left(\frac{u^2}{4} - ab(p_e - p)\right) > 0. \end{aligned}$$

The last inequality is due to (H2), from which $\frac{u^2}{4} > ab(p_e - p)$ on $\mathcal{C}$. Thus is also valid on $\mathcal{F}_s$ where λ is larger compared to point on $\mathcal{C}$ with the same u. So the flow on the slant side $\mathcal{F}_s$ must leave W.

Since $d\lambda/d\xi = (u\theta)/(bm) > 0$, the flow on $\mathcal{F}_r$ must leave W.

Let $\mathcal{F}_b = \mathcal{F}_{b1} \cup \mathcal{F}_{b2}$, where $\mathcal{F}_{b1}$ consists of points where $p < p_e$.

Since $d\theta/d\xi = -ab(p_e - p)\lambda(1-\lambda)m/u < 0$, the flow on the bottom side $\mathcal{F}_{b1}$ must leave W, while the flow on the side $\mathcal{F}_{b2}$ must enter W.

On the front side $\mathcal{F}_f$, if $\lambda = 0$, then $du/d\xi = m(u - u_-) + (p - p_-) = 0$. If $\lambda > 0$, due to $P^m_\lambda > 0$, we have $du/d\xi > 0$. The flow on $\mathcal{F}_f$ must enter W.

On the back side $\mathcal{F}_k$, the vector field $\mathbf{f}$ satisfies $\lambda' > 0, u' = 0$ and the inward normal is $(1, 0, -d\lambda^c/du)$. Thus $\mathbf{f} \cdot \mathbf{n} > 0$. The flow on $\mathcal{F}_k$ must enter W.

It is also straightforward to check that the flow cannot enter W through the nine edges of W. We have proved the following lemma.

LEMMA 4.5. *There are two mutually disjoint open sets $G_1 = \mathcal{F}_s \cup \mathcal{F}_r, G_2 = \mathcal{F}_{b1}$ on the surface of W where any trajectory starting on W can leave W only through G_1, G_2. There are two mutually disjoint open sets $I_1 = \mathcal{F}_f, I_2 = \mathcal{F}_b$ on the surface of W where any trajectory starting on W can leave W only through I_1 and I_2.*

Thus the backward flow can leave W only through the sides $\mathcal{F}_k$ and $\mathcal{F}_f \cup \mathcal{F}_{b2}$.

Based on the eigenvectors, the local stable manifold can be expressed as

$$\theta = \theta^s(\lambda, u), \quad 1-\delta < \lambda \le 1,\ u_+ - \delta < u < u_+ + \delta.$$

Recall that the isocline $\mathcal{C} := \{\lambda = \lambda^c(u)\}$ with $\lambda^c(u_+) = 1$. Let $\delta_1 < \delta$ be a small positive number such that $\lambda^c(u_+ - \delta_1) > \lambda^c(u_+) - \delta = 1 - \delta$. Consider a short segment on $W^s_{loc}(E_+)$ defined as

$$\overline{P_1P_2} := \{(\lambda, \theta, u) : u = u_+ - \delta_1, \lambda^c(u_+ - \delta_1) < \lambda < 1, \theta = \theta^s(\lambda, u)\},$$

where P_1 corresponds to $\lambda = \lambda^c(u_+ - \delta_1)$ and P_2 corresponds to $\lambda = 1$. The flow $\Phi(\xi, P_1), \xi \le 0$, leaves W through the vertical surface supported by $\mathcal{C}$. The flow $\Phi(\xi, P_2), \xi \le 0$, leaves W along the line $\lambda = 1, u = u_-$. The two open sets are mutually disjoint. Therefore, there exists at least one point $P \in \overline{P_1P_2}$ such that $\Phi(\xi, P) = (\lambda(\xi), \theta(\xi), u(\xi), \xi \le 0$, stays in W for all $\xi \le 0$. Clearly the $\lambda(\xi)$ and $u(\xi), \xi \le 0$, are bounded and monotone. Similar to the proof of Theorem 4.2, we can show that the alpha limit set of $\Phi(\xi, P)$ is the unique equilibrium point E_- on the boundary of W. Also, the heteroclinic orbit is monotone in its λ, u components.

5. Numerical computation of the transverse heteroclinic orbits. In this section, we present numerical computation of the heteroclinic solutions connecting E_- to E_+. In the subsonic case, the numerical simulation also shows that the heteroclinic orbit is a transverse intersection of $W^u(E_-)$ and $W^s(E_+)$.

Consider the supersonic internal layer first. From Table 1, $\dim W^u(E_-) = 3$ and $\dim W^s(E_+) = 1$. Therefore, the corresponding heteroclinic orbit whose existence is proved in Theorem 4.2 represents a transverse intersection of $W^u(E_-)$ and $W^s(E_+)$. On the one-dimensional tangent space of $W^s_{loc}(E_+)$, we pick a point P that is sufficiently close to E_+ and compute its orbit backward in time. Although P is not exactly on $W^s_{loc}(E_+)$, the distance is of higher order to the distance $d(P, E_+)$. Also, due to the hyperbolicity of E_+, $W^s_{loc}(E_+)$ is locally backward attracting the numerical orbit so the error is further reduced in backward time.

Numerical simulation of the heteroclinic solution is shown in Figure 5.1. We choose the pressure to be $p = (1+\lambda)\rho^2$. For convenience let $p_e = 1, a = 0.4$, and $b = 0.8$. The heteroclinic solution connects $\lambda_- = 0, \rho_- = 0.5071, u_- = 2.3927, p_- = 0.2572$ to $\lambda_+ = 1, \rho_+ = 0.6071, u_+ = 2.0023, p_+ = 0.7372$. The sound speeds $\sqrt{\partial p/\partial \rho}$ are 0.8426 and 1.3054 at the minus and plus ends of the heteroclinic solution, verifying that the wave is supersonic. As predicted in section 4, $u(\xi)$ is a decreasing function of ξ.

In the rest of this section we consider the subsonic internal layer solution. From Table 1 again, we have $\dim W^u(E_-) = \dim W^s(E_+) = 2$. Generically these two manifolds should intersect transversely in $\mathbb{R}^3$. We are not able to prove such result analytically. The alternative is to numerically show the intersection is transversal. However, we find that although the existence of heteroclinic orbit has been proved, computing the heteroclinic orbit numerically seems to be a nontrivial task. One of

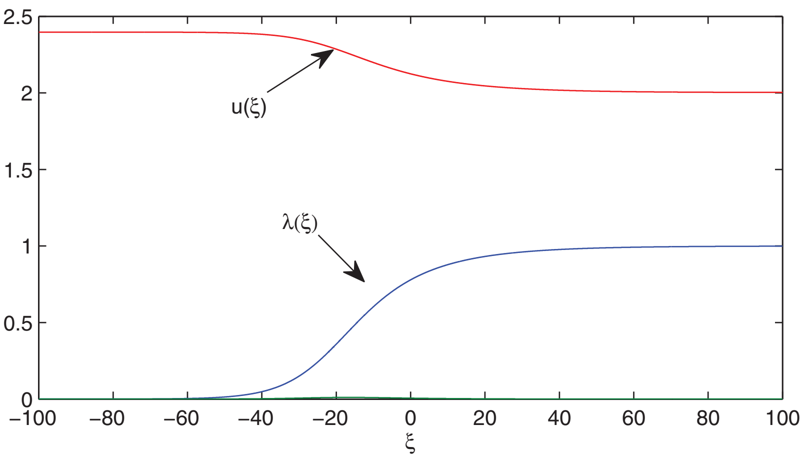

FIG. 5.1. *Supersonic waves (u, λ) in the fast time $\xi = (r - r_0)/\epsilon$.*

the purposes of this section is to introduce a *multistep bidirectional shooting method* for computing such orbit.

We compute the numerical heteroclinic solution by our method for the pressure function $p = (1 + \lambda)\rho^2$, $p_e = 1, a = 1, b = 0.5$. The heteroclinic solution connects $\lambda_- = 0, \rho_- = 0.9615, u_- = \underline{0.5438}, p_- = 0.9246$ to $\rho_+ = 0.6195, u_+ = 0.8441, p_+ = 0.7676$. The sound speeds $\sqrt{\partial p/\partial \rho}$ are 1.3868 and 1.5742 at the minus and plus ends of the heteroclinic solution, verifying that the wave is subsonic. Figure 5.2 shows the phase portrait of u and θ against λ. As predicted in section 4, $u(\xi)$ is an increasing function of ξ.

We now introduce the numerical method that computes the heteroclinic orbit and also shows it is a transverse heteroclinic orbit. The idea is illustrated in Figure 5.3.

A bidirectional shooting method that does not work. As in the proof of the existence of the heteroclinic orbit by the shooting method, we would like to find two extremely close points A_{01}, A_{02} on $W^u_{loc}(E_-)$ such that the trajectories through A_{01} and A_{02} leave W at two disjoint egress sets of W. Then there is a true orbit starting somewhere between A_{01} and A_{02}. We hope to use this approximation up to $\lambda = 0.5$. We would like to similarly find two extremely close points on $W^s_{loc}(E_+)$ such that the backward trajectories through them leave W on two disjoint ingress sets of W. Then there is a true orbit starting somewhere between those points and on $W^s(E_+)$. We hope to use this approximation backward up to $\lambda = 0.5$. The union of the two pieces of numerical orbits should be a good approximation of the heteroclinic orbit.

However, the real numerical computation shows that such an intuitive idea may not work. The flow expands too fast. Even if A_{01} and A_{02} are extremely close to each other ($< 10^{-14}$), the trajectories through them hit the egress sets after a time that is too short for the λ value to advance to $\lambda = 0.5$. See Figure 5.4. The same trouble appears on the backward flow from E_+ to E_-.

Intuitive idea of the multiple-step bidirectional shooting method. To avoid letting the trajectories split too far away we use k-Poincaré sessions in the (λ, θ, u) phase space, illustrated in Figure 5.3.

$$\Lambda_j := \{(\lambda, \theta, u) | \lambda = \lambda_j\}, \quad 0 < \lambda_0 < \lambda_1 < \cdots < \lambda_k < 1.$$

We choose λ_0 and λ_k very close to 0 and 1, respectively, and $|\lambda_j - \lambda_{j-1}|$ is not too large.

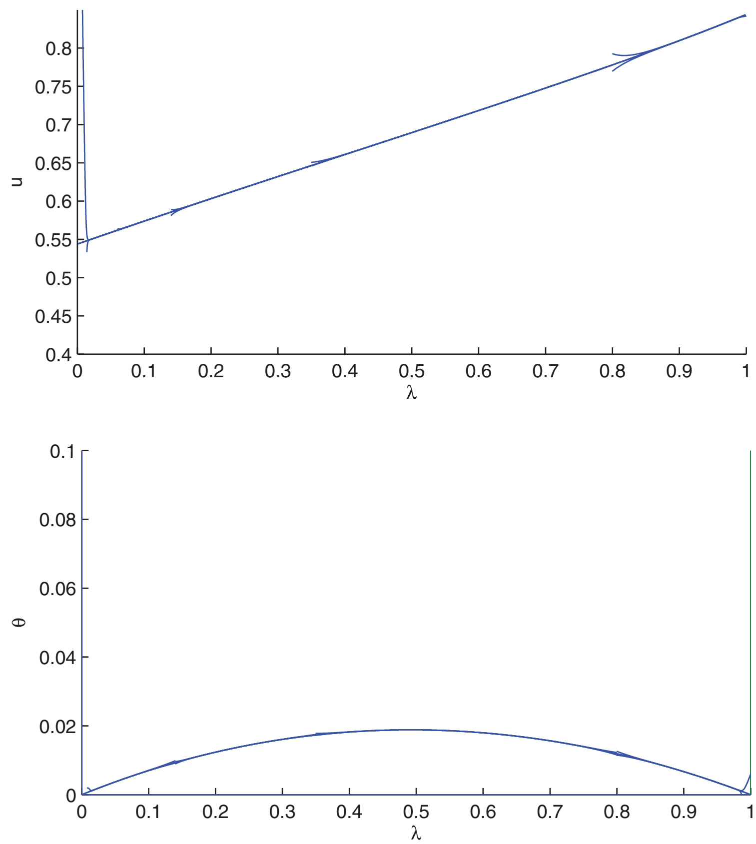

FIG. 5.2. *A subsonic wave in the phase planes* (λ, u) *and* (λ, θ). *They are represented by a sequence of forward and backward expanding wedges, plotted together. The lines with large slope in the upper and lower pictures show that the solutions can expand rapidly either backward or forward in time if not truncated.*

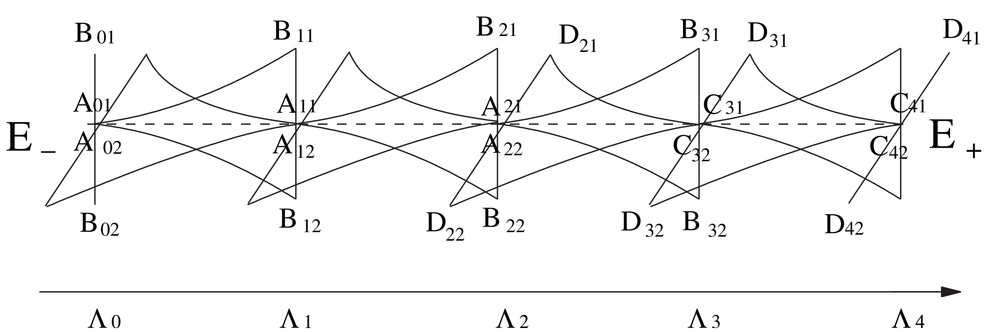

FIG. 5.3. *The figure shows a sequence of forward expanding wedges from* E_- *to* E_+ *and a sequence of backward expanding wedges from* E_+ *to* E_-. *To avoid cloudiness, not all variables are labeled. The intersection of forward and backward wedges is the approximation of a true heteroclinic orbit, shown in the figure as a dotted line.*

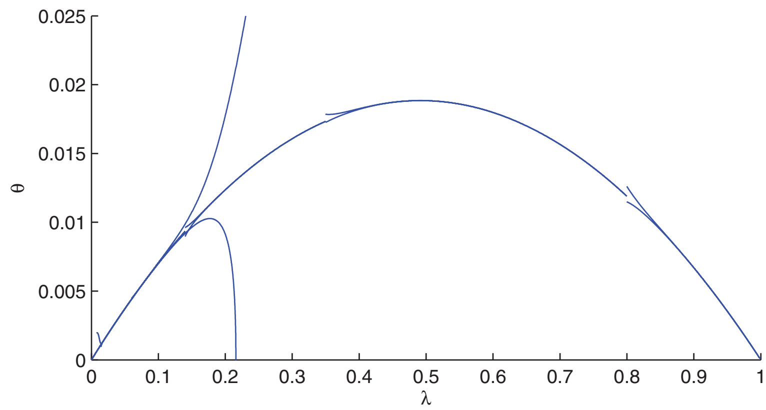

FIG. 5.4. *Plot of a subsonic wave in the phase plane* (λ, θ). *This figure shows that solutions are very sensitive to the change of initial conditions. We have to use the forward and backward shooting several time to draw the figure.*

The precise location and the total number k will be determined "by hand." In our case $k = 4$. Let $\Pi : \Lambda_j \to \Lambda_{j+1}$ be the Poincaré mapping induced by the flow of (4.1).

We now construct a sequence of forward expanding wedges from Λ_0 to Λ_4 as follows. Let B_{01}, B_{02} be two points on $TW^u_{loc}(E_-) \cap \Lambda_0 \cap W$ such that the orbits through them hit disjoint egress sets of W. By refining the interval, we find two extremely close ($\approx 10^{-14}$) points A_{01}, A_{02} on the line segment $\overline{B_{01}B_{02}}$, such that the orbits through them hit disjoint egress sets of W. Define $B_{11} = \Pi(A_{01}), B_{12} = \Pi(A_{02})$ on Λ_1. Since $\lambda_1 - \lambda_0$ is small, B_{11}, B_{12} are in W. Numerically we see that $d(B_{11}, B_{12}) >> d(A_{01}, A_{02})$. We call $(A_{01}A_{02}B_{11}B_{12})$ *a forward expanding wedge.*

On the line segment $\overline{B_{11}B_{12}}$ on Λ_1, we use the "method of bisecting interval" to find two extremely close points A_{11}, A_{12}; through them the orbits hit distinct egress sets again. Let $B_{21} = \Pi(A_{11}), B_{22} = \Pi(A_{12})$ on Λ_2. Repeating the process, eventually we get two extremely close points A_{31}, A_{32} on Λ_3 whose Poincaré images are B_{41}, B_{42} on Λ_4. We finally obtain two points A_{41}, A_{42} on Λ_4, such that the orbits through them hit disjoint egress sets of W. This time they are sufficiently close to E_+. So the forward expanding wedges have been constructed.

We make two comments about our approach. First, the orbits starting between A_{01}, A_{02} do not form a straight line when hitting the Poincaré plane Λ_1. Since we cannot improve this numerically, we have to approximate it by a straight line segment $\overline{B_{11}, B_{12}}$. Second, the pair of points that form the tips of the forward wedges, $A_{j1}, A_{j2}, j = 0, \dots, 4$, are almost on the two-dimensional stable manifold $W^s(E_+)$ by the principle of the shooting method, but the shooting method does not guarantee that $A_{j1}, A_{j2}, j = 0, \dots, 4$, are close to any single orbit on $W^s(E_+)$. And we do not know if they are close to the manifold $W^u(E_-)$.

The remedy is to construct backward expanding wedges from Λ_4 to Λ_0. First D_{41}, D_{42} are two points on $\Lambda_4 \cap TW^s_{loc}(E_+) \cap W$ with the property that the backward orbits through them hit disjoint ingress sets of W. Let $\Phi : \Lambda_j \to \Lambda_{j-1}$ be the Poincaré mapping induced by the backward flow of (4.1). On each Λ_j we find two extremely close points C_{j1}, C_{j2} on $\overline{D_{j1}D_{j2}}$, such that the backward orbits through them hit disjoint ingress sets of W. Let $D_{j-1,1} = \Phi(C_{j1}), D_{j-1,2} = \Phi(C_{j2})$ on Λ_{j-1}. Since $\lambda_j - \lambda_{j-1}$ is small, $D_{j-1,1}$ and $D_{j-1,2}$ are both in W. Assume that $d(D_{j-1,1}, D_{j-1,2}) >> d(C_{j1}, C_{j2})$. Joining $D_{j-1,1}$ and $D_{j-1,2}$ by a line segment, we have a sequence of

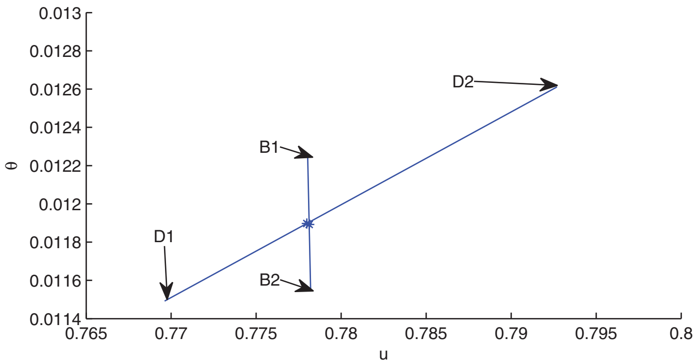

Fig. 5.5. *$\overline{B_{j1}B_{j2}}$ is the longer base of the forward wedge and $\overline{D_{j1}D_{j2}}$ is the longer base of the backward wedge on Λ_j. They intersect transversely on Λ_j.*

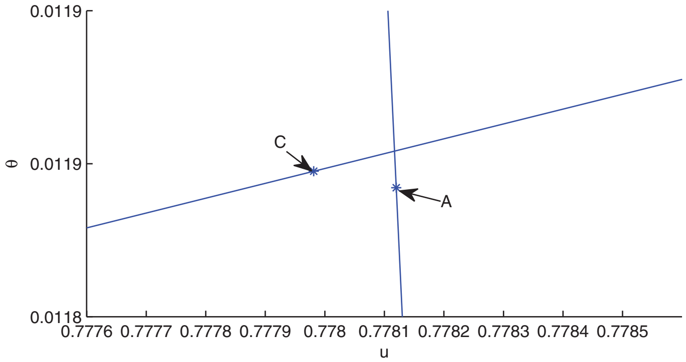

Fig. 5.6. *The zoomed view of Figure 5.5. Point A represents two points A_{j1}, A_{j2} on $\overline{B_{j1}B_{j2}}$, and C represents two points C_{j1}, C_{j2} on $\overline{D_{j1}D_{j2}}$, too close to tell the difference. The intersection of two lines is approximately a point on the heteroclinic orbit.*

backward expanding wedges $(C_{j1}C_{j2}D_{j-1,1}D_{j-1,2})$. Finally, on $\overline{D_{0,1}D_{0,2}}$ we find two close points C_{01}, C_{02} such that the orbits through them exit W from disjoint ingress sets. Both C_{01}, C_{02} are approximately on $W^u_{loc}(E_-)$ and close to E_-. This completes the backward shooting process.

From the numerical computation, we observe that the wedges we constructed have the following properties:

(T1) All the forward and backward wedges are expanding, i.e.,

$$d(A_{j-1,1}, A_{j-1,2}) << d(B_{j1}, B_{j2}) \quad \text{and} \quad d(C_{j1}, C_{j2}) << d(D_{j-1,1}, D_{j-1,2}).$$

(T2) The tips of the forward and backward expanding intervals are δ-close, i.e., $|A_{j1} - C_{j1}| \le \delta,\ j = 0, \dots, m$, where $\delta > 0$ is a small positive constant.

(T3) On each Λ_j, the line segments $\overline{B_{j1}B_{j2}}$ and $\overline{D_{j1}D_{j2}}$ intersect transversally on a point that is close to both $\overline{A_{j1}A_{j2}}$ and $\overline{C_{j1}C_{j2}}$.

The evidence of (T1) is presented in Figures 5.4 and 5.2. For (T2) and (T3) see Figure 5.5 and the zoomed view Figure 5.6.

We now construct a piecewise continuous approximation of the heteroclinic orbit $E_- \to E_+$ as follows.

We first fill in the interior points for the wedges which are only hollow frames so far. For each $\bar\lambda \in (\lambda_j, \lambda_{j+1})$, the orbit $\widehat{A_{j\ell}B_{j+1,\ell}}$ intersects the plane $\lambda = \bar\lambda$ transversely at a unique point $Q_\ell(\bar\lambda), \ell = 1, 2$. The backward orbit $\widehat{C_{j+1,\ell}D_{j\ell}}$ intersects the plane $\lambda = \bar\lambda$ transversely at a unique point $R_\ell(\bar\lambda), \ell = 1, 2$. Connecting by line segments, we fill in the forward and backward expanding wedges by line segments as

$$\mathcal{W}_j^f = \cup\{\overline{Q_1(\bar\lambda)Q_2(\bar\lambda)} \mid \lambda_j < \bar\lambda < \lambda_{j+1}\},$$
$$\mathcal{W}_j^b = \cup\{\overline{R_1(\bar\lambda)R_2(\bar\lambda)} \mid \lambda_j < \bar\lambda < \lambda_{j+1}\}.$$

If $\lambda_j - \lambda_{j-1}$ is sufficiently small, then the property (T3) on Λ_j and Λ_{j+1} should imply that all the lines $\overline{Q_1(\lambda)Q_2(\lambda)}$ and $\overline{R_1(\lambda)R_2(\lambda)}$ intersect transversely for each $\lambda \in (\lambda_j, \lambda_{j+1})$.

We now define the pseudo orbit $q_j(\lambda)$ between Λ_j, Λ_{j+1} as the transversal intersection of $\mathcal{W}_j^f \cap \mathcal{W}_j^b$. In the process of refining the intervals and computing solutions forward and backward on many partition points of the intervals $\overline{B_{j1}B_{j2}}$ and $\overline{D_{j1}D_{j2}}$ we find numerically that the orbits near the pseudo orbit $q_j(\lambda)$ are rapidly splitting, forward or backward, in two transversal directions. We argue that the linear variational system around the orbit $q_j(\lambda)$ has exponential dichotomy on the subinterval $[\lambda_j, \lambda_{j+1}]$. We shall assume that this is a fact for our system. Then the following rigorous result about our system can be proved.

THEOREM 5.1. *Assume* (1) *the linear variational system around the pseudo orbit* $q_j(\lambda), \lambda_j \le \lambda \le \lambda_{j+1}$ *has an exponential dichotomy for each* $j = 0, \dots, k-1$; (2) *the distance* $\lambda_{j+1} - \lambda_j$ *is sufficiently small;* (3) *the intersections of the bases of the forward and backward the wedges are transversal; and* (4) *the constant* δ *as in* (T2) *is sufficiently small. Then there is an exact heteroclinic orbit near the pseudo orbit* $q_{approx}(\lambda) = \cup_{j=1}^m \{q_j\}$. *Moreover, the intersections of* $W^u(E_-)$ *and* $W^s(E_+)$ *are transversal along the heteroclinic orbit.*

The proof of the existence of an exact heteroclinic orbit q_{ex} near the pseudo orbits $\{q_j\}, j = 0, \dots, k-1$, is often referred as the "shadowing lemma for flows"; cf. [34, 35] and many other publications. To show the heteroclinic orbit q_{ex} is a transverse heteroclinic orbit, first observe by the roughness of the exponential dichotomies that the linear variational system around q_{ex} has an exponential dichotomy on each subinterval $[\lambda_j, \lambda_{j+1}]$, and the unstable subspace for the previous interval and the stable subspace for the next interval intersect transversely on each $\Lambda_j, j = 1, \dots, k-1$. It is easy to define a unified exponential dichotomy around q_{ex} for all $\xi \in \mathbb{R}$. Details will be left to the reader.

6. Existence of a real solution near the approximation. We have constructed solutions of the slow system $n_j(s), j = 1, 2$, and the heteroclinic solution $(\lambda, \theta, u)(\xi), \xi \in \mathbb{R}$ of the fast system. Let $Y(x) = (r(x), n(x), u(x), \lambda(x), \theta(x))$ be a vector valued function from $[r_1, r_2] \to \mathbb{R}^5$. Define $Y_j(s), j = 1, 2$, on I_j as follows:

$$Y_j(s) := (r_j(s), n_j(s), u_j(s), \lambda_j(s), \theta_j(s)) \text{ for } s \in I_j, j = 1, 2,$$
$$\text{where } \lambda_1(s) = 0, \lambda_2(s) = 1, \theta_j = 0, u_j(s) = u^{\pm}(m(s), n(s), \lambda_j).$$

Define $Y_0(\xi) := (r_0, n_0, u(\xi), \lambda(\xi), \theta(\xi))$ on $I_0(\xi)$ which in the fast time ξ is $(-\infty, \infty)$. See (1.5) and (1.6) for the relation between I_0 and $I_0(\xi)$.

Then $Y_j(s), j = 1, 2$, satisfies the slow system (2.3) and $Y_0(\xi)$ satisfies the fast system (2.4) when $\epsilon = 0$. When $\epsilon > 0$ and small, $Y_j(s)$ satisfies (2.3) approximately and $Y_0(\xi)$ satisfies (2.4) approximately with $o(1)$ residual errors as $\epsilon \to 0$.

Recall the definition of three layers in (1.5). An approximation $Y_{ap} = (r_{ap}, n_{ap}, u_{ap}, \lambda_{ap}, \theta_{ap})$ for all $s \in [r_1, r_2]$ can be defined as follows.

DEFINITION 6.1. *If $s \in I_j, j = 1, 2$, then let $Y_{ap}(s) := Y_j(s)$, while if $s \in I_0$, then let $Y_{ap}(s) := Y_0((s - r_0)/\epsilon)$.*

We remark that Y_{ap} has $o(1)$ jump errors at $r_0 \pm \eta$ if $\epsilon \to 0$, due to the matching conditions (2.7).

The purpose of this section is to show under suitable boundary conditions on the two ends of the nozzle, for small nonzero ϵ, that the singularly perturbed system (1.3) has a unique standing wave solution $Y(s)$ near the approximation $Y_{ap}(s), s \in [r_1, r_2]$.

It is desirable to consider the problem in a general abstract setting. First we summarize properties satisfied by the singular limit systems (2.5) and (2.6) and the approximations Y_{ap}. Then we propose some boundary conditions on the system so that the exact standing wave solution near the approximation Y_{ap} can exist.

(P1) The two branches of the slow manifolds, $S_0^{\pm}$ and $S_1^{\pm}$, as in (3.2), consist of normally hyperbolic equilibrium points of the last three equations of (2.6). That is, all the eigenvalues at $S_j^{\pm}, j = 0, 1$, have nonzero real parts.

(P2) There exists an open set $O_0 \subset \mathbb{R}^2$ such that if $(r_0, n_0) \in O_0$, then with (r_0, n_0) as a parameter, the last three equations of system (2.6) have a transversal heteroclinic orbit, i.e., it is the transverse intersection of $W^u(E_-)$ and $W^s(E_+)$, where $E_- \in S_0^{\pm}$ and $E_+ \in S_1^{\pm}$.

(P3) There exist two open sets O_1 and O_2 in $\mathbb{R}$ such that if $n_{j0} \in O_j$ is the initial data, the two trajectories $n_j(s)$ of (3.10) and (3.11) intersect transversely at the jump point $(r, n) = (r_0, n_0) \in O_0$.

We remark that the normal hyperbolicity of $S_j^{\pm}, j = 1, 2$, in (P1) is based on the signs of eigenvalues as in Table 1. In section 4, we established the existence of heteroclinic solutions for both subsonic and supersonic cases for the parameter (r_0, n_0). The numerical simulation in section 5 shows that some of the heteroclinic orbits are transversal heteroclinic orbits. If (r_0, n_0) is a parameter so that a transverse heteroclinic orbit exists, then there exists an open set O_0 containing (r_0, n_0) such that for all $(\bar{r}_0, \bar{n}_0) \in O_0$, there exists a transverse heteroclinic orbit for (2.6). That verifies (P2). Finally, if conditions in Lemma 3.5 are satisfied and $n_j(s), j = 1, 2$ are smooth solutions of (3.10) and (3.11) for $j = 1, 2$, respectively, which satisfy $n_2(r_0+) = n_1(r_0-)$, then let $n_{10} = n_1(r_1), n_{20} = n_2(r_2)$. There exist open sets O_1 containing n_{10} and open set O_2 containing n_{20} such that O_1 and O_2 satisfy property (P3). The transverse intersection of trajectories $n_j(s), j = 1, 2$, as in (P3) is proved in Lemma 3.4.

Let us express the boundary conditions at the two ends of the nozzle as

$$(r, n, u, \lambda, \theta) \in B_j, \ j = 1, 2,$$

where $B_j, j = 1, 2$, are smooth manifolds of dimensions $d_j, j = 1, 2$, respectively. To avoid boundary layers, we shall assume that B_j passes through the equilibrium point on S_j whose first two coordinates are (r_j, n_{j0}). When $\epsilon > 0$ and small, the slow manifold is $O(\epsilon)$ to its singular limit, but the boundary conditions do not change with ϵ. Thus there will be boundary layers of the size $O(\epsilon)$ at the two ends of the nozzle.

Let $T(s, P, \epsilon)$ be the solution map for (2.3). Consider all the orbits starting from $B_j, j = 1, 2$. They form two smooth manifolds of dimensions $d_j + 1, j = 1, 2$:

$$M_j = T(s, B_j, \epsilon), s_1 \leq s \leq s_2.$$

The general idea from the dynamical systems is as follows: for small positive ϵ, if the two solution manifolds M_1 and M_2 intersect transversely along a one-dimensional

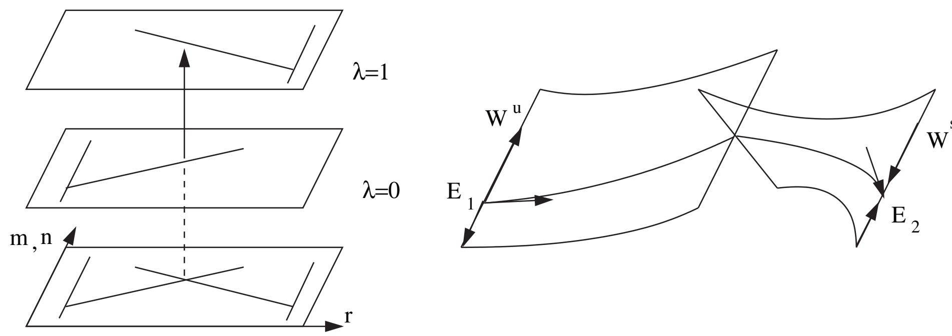

FIG. 6.1. *Left: transversal intersection of the slow flows on the slow manifolds $\lambda = 0$ and $\lambda = 1$. Right: transversal intersection of the unstable and stable manifolds along the heteroclinic orbit.*

curve, then the intersection is the unique solution of the boundary value problem. Using the geometric theory of singular perturbations, such a transversal intersection can be checked on the slow and fast limiting systems as follows.

From (P1), each point on the slow manifold, as an equilibrium point, has a unique stable manifold and a unique unstable manifold passing through it. The union of all the stable (or unstable) manifolds over all the points of the slow manifolds S_j form the center-stable manifolds $W^{cs}(S_j)$ (or the center-unstable manifolds $W^{cu}(S_j)$).

$$W^{cs}(S_j) := \bigcup\{W^s(P) : P \in S_j\},$$
$$W^{cu}(S_j) := \bigcup\{W^u(P) : P \in S_j\}.$$

If the solutions to (3.10) and (3.11), $(r_j(s), n_j(s))$, intersect at (r_0, n_0), then from Lemma 3.4, the intersection of the curves $(r_j(s), n_j(s))$ is transversal. This gives the desired transverse intersection condition for the slow variables governed by system (2.5).

If (P2) is satisfied, then there exists an open set O_0 such that if $(r, n) \in O_0$, then the fast system (4.1) has a transverse heteroclinic orbit connecting equilibrium points on the two slow manifolds. This is the desired transverse condition for the fast variables governed by the fast system (2.6).

The transverse intersection of limiting manifolds ($\epsilon = 0$) in slow variables and fast variables is depicted in Figure 6.1.

We need some conditions on the boundary manifolds:

(H4) For the subsonic case, assume that the dimensions of the boundary manifolds B_1 and B_2 are $d_1 = d_2 = 2$. For the supersonic case, assume that $d_1 = 3, d_2 = 1$. Furthermore, assume that the boundary manifold B_1 and the center-stable manifold $W^{cs}(S_0)$ intersect transversely at a unique point P_1. The boundary manifold B_2 and the center-unstable manifold $W^{cu}(S_1)$ intersect transversely at a unique point P_2. The points P_1, P_2 are defined as

$$P_1 = \{(r_1, n_{10}, u = u^{\pm}(m(r_1), n_{10}, \lambda = 0)), \lambda = 0, \theta = 0\},$$
$$P_2 = \{(r_2, n_{20}, u = u^{\pm}(m(r_2), n_{20}, \lambda = 1)), \lambda = 1, \theta = 0\},$$

THEOREM 6.2. *Given that for $\epsilon = 0$, the singular limiting systems* (2.5) *and* (2.6) *and the limiting singular orbits satisfy conditions* (P1) *to* (P3)*, then if the boundary conditions satisfy* (H4)*, there exists a supersonic or subsonic standing wave near the approximation Y_{ap} for each sufficiently small positive ϵ.*

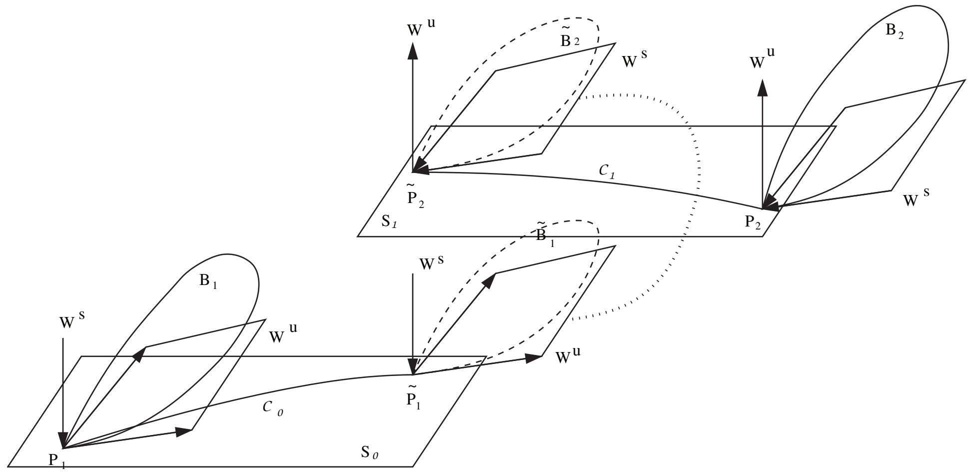

FIG. 6.2. *The dotted line indicates the transversal intersection of the unstable manifold of $\tilde{P}_1$ and the stable manifold of $\tilde{P}_2$. For small ϵ, under the flow of* (2.4)*, the image of B_1 is $\tilde{B}_1$ and the backward image of B_2 is $\tilde{B}_2$. They also intersect transversally.*

Proof. There are two equivalent methods to prove the theorem: the analytic method and the geometric method. We only outline the proofs since both methods are now standard.

The most convenient way to prove the existence of a true solution near the singular limit solution is the geometric method. The geometric method tracks the trajectories of the boundary manifolds B_1 and B_2 under the flow of (2.3) or (2.4) to see if they intersect transversally. If this is the case, then the intersection uniquely determines the true solution near the singular orbit.

To illustrate the idea of the proof, consider the case of subsonic waves. At $\epsilon = 0$, let $\mathcal{C}_0$ be the trajectory of P_1 under the flow on the slow manifold S_0, and let $\mathcal{C}_1$ be the trajectory of P_2 under the flow on the slow manifold S_1. Based on our assumption, the projections of $\mathcal{C}_0$ and $\mathcal{C}_1$ to the slow variables (r, n) intersect at a point $P_0 = (r_0, n_0)$, whose preimages of the projections are $\tilde{P}_1$ on S_0 and $\tilde{P}_2$ on S_1. See Figure 6.2 and the left graph of Figure 6.1.

Since the slow manifold S_0 consists of hyperbolic equilibrium points, each is attached by a one-dimensional stable manifold and a two-dimensional unstable manifold; the slow manifold S_1 consists of hyperbolic equilibrium points, each attached by a one-dimensional unstable manifold and a two-dimensional stable manifold. The union of such unstable manifolds over the curve $\mathcal{C}_0$ is a three-dimensional submanifold of $W^{cu}(S_0)$, and the union of such stable manifolds over the curve $\mathcal{C}_1$ is a three-dimensional submanifold of $W^{cs}(S_1)$. Denote them by $\tilde{W}^{cu}(S_0)$ and $\tilde{W}^{cs}(S_1)$, respectively.

Observe that the curves $\mathcal{C}_0$ and $\mathcal{C}_1$ intersect transversally when projected to the (r, n) plane. Furthermore, $W^u(\tilde{P}_1)$ intersects transversally with $W^s(\tilde{P}_2)$, depicted as the dotted line in Figure 6.2. See also Figure 6.1. Base on this, it is clear that the two three-dimensional submanifolds $\tilde{W}^{cu}(S_0)$ and $\tilde{W}^{cs}(S_1)$ intersect transversally in the five-dimensional phase space.

Now the boundary manifold B_1 transversally intersects $W^{cs}(S_0)$ at a point $P_1 \in S_0$, and the boundary manifold B_2 transversally intersects $W^{cu}(S_1)$ at a point $P_2 \in S_1$. According to the "lambda lemma," or the "inclination lemma" [20, 11], the boundary manifold B_1 will follow the direction of the flow on $W^s(P_1)$ in forward time, and B_2 will follow the direction of the flow on $W^u(P_2)$ in backward time to approach the equilibrium points P_1, P_2 exponentially. Moreover, the tangent planes of the boundary manifolds will approach the tangent planes of the unstable and stable manifolds of the equilibrium points P_1, P_2 respectively. See Figure 6.2.

Those facts will be preserved if $\epsilon > 0$ is sufficiently small. The slow manifolds S_j becomes two nearby "center manifolds" $S_j(\epsilon)$ [19]. The center-stable fiber at $P_1(\epsilon) \in S_0(\epsilon)$ intersects with B_1 transversely. The center-unstable fiber at $P_2(\epsilon) \in S_1(\epsilon)$ intersects with B_2 transversely. To avoid overcrowdedness, we did not plot $P_j(\epsilon)$ and $S_j(\epsilon)$. Rather we substitute them with P_j and S_j in Figure 6.2. Similarly, the curve $\mathcal{C}_j$ now becomes a nearby curve $\mathcal{C}_j(\epsilon)$. Near the interior point $P_0 = (r_0, n_0)$, the center unstable fibers of $S_0(\epsilon)$ transversely intersect the center stable fibers of $S_1(\epsilon)$, as from Lemma 3.4 and (P2), since the transversal intersection of manifolds does not go away under small perturbations.

When $\epsilon > 0$, the points on the slow manifolds are no longer stationary. They move slowly according to the slow system (2.3). The boundary manifolds B_1, B_2 will also move under the slow flow. Meanwhile the image of B_1 will approach the unstable fibers of the slow manifold $S_0(\epsilon)$ to the position $\tilde{B}_1$ that is based on $\tilde{P}_1$. The image of B_2 will approach the stable fiber of the slow manifold $S_1(\epsilon)$ to the position $\tilde{B}_2$ that is based on $\tilde{P}_2$. This process is described by the exchange lemmas [22, 4, 36]. Under the flow of (2.4), the images of the two boundary manifolds, $\tilde{B}_1$ and $\tilde{B}_2$, are C^1 close to the unstable and stable fibers of the slow manifolds at $\tilde{P}_1$ and $\tilde{P}_2$. Therefore, they intersect transversally. The true solution is locally uniquely determined by such transversal intersection.

Next we describe the analytic method, which may also be called the "error correction method." Recall the approximation of the standing wave

$$Y_{ap} = (r_{ap}, n_{ap}, u_{ap}, \lambda_{ap}, \theta_{ap}) \text{ on } [r_1, r_2].$$

Since r_{ap} is exact, the true solution can be expressed as

$$Y = (r_{ap}, n_{ap} + \Delta n, u_{ap} + \Delta u, \lambda_{ap} + \Delta\lambda, \theta_{ap} + \Delta\theta).$$

Then the linear variational system for the correction terms $(\Delta n, \Delta u, \Delta\lambda, \Delta\theta)$ is

$$L(\Delta n, \Delta u, \Delta\lambda, \Delta\theta, \epsilon) = -\Delta f, \tag{6.1}$$

where L is a linear operator that includes the linearized differential equations and the evaluation of the jumps at the junction points $r_0 \mp \eta$ between I_1, I_0, and I_2. Δf represents the residual and jump errors of the approximation. The iteration method in suitable functional spaces can be used to obtain the correction terms of this linear system. Then the nonlinear system for the correction terms can be obtained a contraction mapping principle.

Solving the linear system (6.1) requires an iteration procedure too. From the singular perturbation theory the slow variables and the fast variables are weakly coupled in the system (6.1); cf. [21, 31]. One can use an approximation of the slow variable Δn to solve for the fast variables $(\Delta u, \Delta\lambda, \Delta\theta)$ first. The solution exists since the linear variational system for the fast equations has exponential dichotomies on each fast and slow layer. One can then use the approximation of fast variables to solve for the slow variable Δn from the slow equation. This time the solution uniquely exists due to the transverse intersection of the trajectories of $(r_1(s), n_1(s))$

and $(r_2(s), n_2(s))$ at (r_0, n_0). The exact solution to the linear variational problem can be obtained by iterating the two steps repeatedly. The parameters (r_0, n_0) also need to be updated in each iteration to help eliminate the jump errors. ∎

The analytic method is based on analyzing a linear system and uses two iteration procedures so it is a little lengthy to carry out. However, the proof also suggests a workable procedure to calculate the true solution near the approximations numerically or asymptotically. Sometimes information on the linear variational system can yield informations on the stability of the standing wave solutions [31].

There are many ways to define the boundary manifolds B_1, B_2 to satisfy the conditions in Theorem 6.2. As mentioned before, to avoid large boundary layers, we assume that B_1 and B_2 pass through S_0 and S_1 when $\epsilon = 0$. When $\epsilon > 0$ and small, the boundary layers are only of the size $O(\epsilon)$. With this in mind we present a choice of boundary conditions as follows.

PROPOSITION 6.3. *The conditions on B_1 and B_2 for the existence of a standing wave solution near Y_{ap} as in Theorem* 6.2 *are satisfied if the following conditions on the (u, λ, θ) components of $B_j, j = 1, 2$, are satisfied:*

(1) *For the subsonic standing wave, let $d_1 = d_2 = 2$. If we define*

$$B_1 := P_1 + \{(0, 0, u, \lambda, \theta) : a_1\lambda + b_1\theta + c_1 u = 0\},$$
$$B_2 := P_2 + \{(0, 0, u, \lambda, \theta) : a_2\lambda + b_2\theta + c_2 u = 0\},$$

then the condition on B_1 is $c_1 \neq 0$ and the condition on B_2 is $(a_2, b_2, c_2)^T \cdot \mathbf{v_2} \neq 0$, where $\mathbf{v_2}$ is the eigenvector corresponding to the unstable eigenvalue $k_2 > 0$; cf. Table 1 *in section* 4.

(2) *For the supersonic standing wave, let $d_1 = 3$ and $d_2 = 1$. If we define*

$$B_1 := P_1 + \{(0, 0, u, \lambda, \theta)\},$$
$$B_2 := P_2 + \{(0, 0, u, \lambda, \theta) : (\lambda, \theta, u) = \tau\mathbf{v}\},$$

where $\mathbf{v}$ is a fixed nonzero vector in $\mathbb{R}^3$ and τ is the coordinate on B_2, then there is no additional condition on B_1, i.e., (λ, θ, u) can be any real numbers. The condition on B_2 is $\det\{\mathbf{v}, \mathbf{v_2}, \mathbf{v_3}\} \neq 0$, *where $\mathbf{v_2}, \mathbf{v_3}$ are eigenvectors corresponding to unstable eigenvalues k_2 and k_3; cf. Table* 1 *in section* 4.

Acknowledgments. The authors thank Martin Wechselberger, Stephen Schecter, and Thomas Ward for stimulating discussions and useful suggestions.

REFERENCES

[1] D. AMADORI AND A. CORLI, *On a model of multiphase flow*, SIAM J. Math. Anal., 40 (2008), pp. 134–166.

[2] D. AMADORI AND A. CORLI, *Global existence of BV solutions and relaxation limit for a model of multiphase reactive flow*, Nonlinear Anal., 72 (2010), pp. 2527–2541.

[3] G. K. BATCHELOR, *An Introduction to Fluid Dynamics*, Cambridge University Press, Cambridge, UK, 2000.

[4] P. BRUNOVSKÝ, *C^r-inclination theorems for singularly perturbed equations*, J. Differential Equations, 155 (1999), pp. 133–152.

[5] S. CANIC, B. L. KEYFITZ, AND G. M. LIEBERMAN, *A proof of existence of perturbed steady transonic shocks via a free boundary problem*, Comm. Pure Appl. Math., 53 (2000), pp. 484–511.

[6] G.-Q. CHEN, S.-X. CHEN, D. WANG, AND Z. WANG, *A multidimensional piston problem for the Euler equations for compressible flow*, Discrete Contin. Dyn. Syst., 13 (2005), pp. 361–383.

[7] S.-X. CHEN, *Compressible flow and transonic shock in a diverging nozzle*, Comm. Math. Phys., 289 (2009), pp. 75–106.

[8] G. Q. Chen, C. M. Dafermos, M. Slemrod, and D. H. Wang, *On two-dimensional sonic-subsonic flow*, Comm. Math. Phys., 271 (2007), pp. 635–647.

[9] A. Corli and H. Fan, *The Riemann problem for reversible reactive flows with metastability*, SIAM J. Appl. Math., 65 (2004), pp. 426–457.

[10] R. Courant and K. O. Friedrichs, *Supersonic Flow and Shock Waves*, Interscience, New York, 1948.

[11] B. Deng, *Homoclinic bifurcations with nonhyperbolic equilibria*, SIAM. J. Math. Anal., 21 (1990), pp. 693–719.

[12] G. Dettelff, P. A. Thompson, G. E. A. Meier, and H.-D. Speckmann, *An experimental investigation of liquefaction shock wave*, J. Fluid Mech., 95 (1979), pp. 279–304.

[13] H. Fan, *Travelling waves, Riemann problems and computations of a model of the dynamics of liquid/vapour phase transitions*, J. Differential Equations, 150 (1998), pp. 385–437.

[14] H. Fan, *Convergence to travelling waves in two model systems related to the dynamics of liquid/vapour phase changes*, J. Differential Equations, 168 (2000), pp. 102–128.

[15] H. Fan, *On a model of the dynamics of liquid/vapor phase transitions*, SIAM J. Appl. Math., 60 (2000), pp. 1270–1301.

[16] H. Fan, *Symmetry breaking, ring formation and other phase boundary structures in shock tube experiments on retrograde fluids*, J. Fluid Mech., 513 (2004), pp. 47–75.

[17] H. Fan and X.-B. Lin, *Collapsing and explosion waves in phase transitions with metastability, existence, stability and related Riemann problems*, J. Dynam. Differential Equations, 22 (2009), pp. 163–191.

[18] H. Fan and X.-B. Lin, *A dynamical systems approach to traveling wave solutions for liquid/vapor phase transition*, Fields Instit. Commun., 61 (2011).

[19] N. Fenichel, *Geometric singular perturbation theory for differential equations*, J. Differential Equations, 31 (1979), pp. 53–98.

[20] J. Guckenheimer, J. Moser, and S. E. Newhouse, *Dynamical Systems*, C.I.M.E. Lectures, Bressanone, Italy, 1978, Birkhäuser, Basel, Switzerland, 1980.

[21] J. Hale and X.-B. Lin, *Multiple internal layer solutions generated by spatially oscillatory perturbations*, J. Differential Equations, 154 (1999), pp. 364–418.

[22] C. K. R. T. Jones and N. Kopell, *Tracking invariant manifolds with differential forms in singularly perturbed systems*, J. Differential Equations, 108 (1994), pp. 64–88.

[23] J. M. Hong, C.-H. Hsu, and W. Liu, *Viscous standing asymptotic states of isentropic compressible flows through a nozzle*, Arch. Ration. Mech. Anal., 196 (2010), pp. 575–597.

[24] J. M. Hong, C.-H. Hsu, and W. Liu, *Inviscid and viscous stationary waves of gas flow through contracting–expanding nozzles*, J. Differential Equations, 248 (2010), pp. 50–76.

[25] W. Liu and M. Oh, *Instability of low density supersonic waves of a viscous isentropic gas flow through a nozzle*, Fields Instit. Commun., to appear.

[26] L. Hsiao, T. Luo, and T. Yang, *Global BV solutions of compressible Euler equations with spherical symmetry and damping*, J. Differential Equations, 146 (1998), pp. 203–225.

[27] G.-S. Jiang and C.-W. Shu, *Efficient implementation of weighted ENO schemes*, J. Comput. Phys., 126 (1996), pp. 202–228.

[28] C. K. R. T. Jones, *Geometric singular perturbation theory*, in Dynamical Systems, Montecatini Terme, 1994, Lecture Notes in Math. 1609, Springer, Berlin, 1995, pp. 44–118.

[29] J. Li, Z. P. Xin, and H. C. Yin, *The existence and monotonicity of a three-dimensional transonic shock in a finite nozzle with axisymmetric exit pressure*, Pacific J. Math., 247 (2010), pp. 109–162.

[30] X.-B. Lin, *Heteroclinic bifurcation and singularly perturbed boundary value problems*, J. Differential Equations, 84 (1990), pp. 319–382.

[31] X.-B. Lin, *Construction and asymptotic stability of structurally stable internal layer solutions*, Trans. Amer. Math. Soc., 353 (2001), pp. 2983–3043.

[32] T.-P. Liu, *Nonlinear stability and instability of transonic flows through a nozzle*, Commun. Math. Phys., 83 (1982), pp. 243–260.

[33] R. O'Malley, *Singular Perturbation Methods for Ordinary Differential Equations*, Appl. Math. Sci. 89, Springer-Verlag, Berlin, 1991.

[34] K. J. Palmer, *Shadowing in Dynamical Systems. Theory and Applications*, Kluwer, Dordrecht, The Netherlands, 2000.

[35] S. Y. Pilyugin, *Shadowing in Dynamical Systems*, Lecture Notes in Math. 1706, Springer-Verlag, Berlin, 1999.

[36] S. Schecter, *Exchange lemmas* 2: *General exchange lemma*, J. Differential Equations, 245 (2008), pp. 411–441.

[37] A. Scheel, *Radially symmetric patterns of reaction-diffusion systems*, Mem. Amer. Math. Soc., 165 (2003).

[38] M. Slemrod, *Resolution of the spherical piston problem for compressible isentropic gas dynamics via a self-similar viscous limit*, Proc. Roy. Soc. Edinburgh Sect. A, 126 (1996), pp. 1309–1340.

[39] P. A. Thompson, G. C. Carofano, and Y.-G. Kim, *Shock waves and phase changes in a large-heat-capacity fluid emerging from a tube*, J. Fluid Mechan., 166 (1986), pp. 57–92.

[40] P. A. Thompson, H. Chaves, G. E. A. Meier, Y.-G. Kim, and H.-D. Speckmann, *Wave splitting in a fluid of large heat capacity*, J. Fluid Mechan., 185 (1987), pp. 385–414.

[41] K. Trivisa, *On the dynamics of liquid-vapor phase transition*, SIAM J. Math. Anal., 39 (2008), pp. 1788–1820.

[42] C. J. Xie and Z. P. Xin, *Global subsonic and subsonic-sonic flows through infinitely long nozzles*, Indiana Univ. Math. J., 56 (2007), pp. 2991–3023.

[43] Z. P. Xin, W. Yan, and H. C. Yin, *Transonic shock problem for the Euler system in a nozzle*, Arch. Ration. Mech. Anal., 194 (2009), pp. 1–47.

[44] T. Yang, *A functional integral approach to shock wave solutions of Euler equations with spherical symmetry*, Commun. Math. Phys., 171 (1995), pp. 607–638.